PAPER • OPEN ACCESS

Field theory of active chiral hard disks: a first-principles approach to steric interactions

To cite this article: Erik Kalz *et al* 2024 *J. Phys. A: Math. Theor.* **57** 265002

View the article online for updates and enhancements.

Field theory of active chiral hard disks: a first-principles approach to steric interactions

Erik Kalz[1,*] ⓘ**, Abhinav Sharma**[2,3] ⓘ **and Ralf Metzler**[1,4] ⓘ

[1] Institute of Physics and Astronomy, University of Potsdam, D-14476 Potsdam, Germany
[2] Institute of Physics, University of Augsburg, D-86159 Augsburg, Germany
[3] Institute Theory of Polymers, Leibniz-Institute for Polymer Research, D-01069 Dresden, Germany
[4] Asia Pacific Centre for Theoretical Physics, KR-37673 Pohang, Republic of Korea

E-mail: erik.kalz@uni-potsdam.de, abhinav.sharma@uni-a.de and ralf.metzler@uni-potsdam.de

Abstract

A first-principles approach for active chiral hard disks is presented, that explicitly accounts for steric interactions on the two-body level. We derive an effective one-body equation for the joint probability distribution of positions and angles of the particles. By projecting onto the angular modes, we write a hierarchy for the lowest hydrodynamic modes, i.e. particle density, polarisation, and nematic tensor. Introducing dimensionless variables in the equations, we highlight the assumptions, which—though inherent—are often included implicit in typical closure schemes of the hierarchy. By considering different regimes of the Péclet number, the well-known models in active matter can be obtained through our consideration. Explicitly, we derive an effective diffusive description and by going to higher orders in the closure scheme, we show that this first-principles approach results in the recently introduced Active Model B +, a natural extension of the Model B for active processes. Remarkably, here

* Author to whom any correspondence should be addressed.

we find that chirality can change the sign of the phenomenological activity parameters.

1. Introduction

The analytic model of an *Active Chiral Particle (ACP)* [1–5] represents an extension to the well-known *Active Brownian Particle (ABP)* model [6–9] with additional active chirality. These models have proven very useful as they come as a first step in generalising equilibrium models to include non-equilibrium, active contributions for microscopic agents. They constitute a minimalist attempt to describe directed motion on the microscale and are found to lead to emerging complex structures on the macroscale. For that reason, they are widely used in the analytic description of non-equilibrium systems [10–12].

The ABP model describes the overdamped motion of a tagged particle influenced by two contributions: firstly, equilibrium fluctuations of the surrounding medium, which give rise to the well-known equilibrium Langevin description. The particle is assumed to diffuse with a spatial diffusion coefficient D_T. Secondly, the particle experiences a non-equilibrium driving force, that might originate from an internal energy depot or external energy input [13–15]. In the simplest case, this scenario is modelled as a self-propulsion with a (constant) velocity v along an orientation vector $\hat{\mathbf{e}}(\theta)$. In the model of an ABP, the self-propulsion direction gets randomised by assuming that the orientation vector additionally is performing rotational diffusion on the unit-sphere with the diffusion coefficient D_R. Despite its simplicity, this 'toy' ABP model has proven tremendously successful in analytical analysis and as a simulation model to describe active matter on a macroscale [16, 17]. Emerging complex macroscopic phases such as motility-induced phase separations [18–23], (chemo-) tactic behaviour [24, 25], flocking [26, 27], or swarming [28–30] have been reported.

The ABP model has been further developed to include active processes that explicitly break the spatial symmetry via an effect of active chirality ω [1–4]. This generalisation in the model allows to describe even more complex emerging phenomena, such as odd viscosity [31, 32], finite-size rotating clusters [33, 34], hyperuniform behaviour [35, 36] and edge currents at interfaces [37–39]. This analytical extension is inspired by experimental observation of bacteria [40–42], sperm cells [43, 44], or syntactical particles [45, 46] as well as macroscopic chiral robots [47–49], which show an archetypal chirality in their trajectories on the microscale. Remarkably, already over a century ago, experimental observations were made in living organisms, which showed that trajectories of certain microorganisms such as *Loxodes* and *Paramecium* break the spatial symmetry and need an interpretation in terms of chiral self-propulsion [50].

An alternative, more coarse-grained viewpoint for describing the emerging complex structures in active systems is based on continuum field-theoretical models of active matter. The starting point is to address the diffusive behaviour of a conserved order parameter, such as the mean particle *probability-density function (PDF)* $\varrho(\mathbf{x}, t)$, where $\varrho(\mathbf{x}, t) \, d\mathbf{x}$ describes the probability of finding a particle in the interval $\mathbf{x}$ and $\mathbf{x} + d\mathbf{x}$ at time t, as in the well-known *Model B* [51]. This model successfully describes the equilibrium behaviour of matter, and especially the dynamics of phase separation [52]. An inherent assumption in the derivation of these field-theoretical models is that the underlying processes follow the detailed-balance dynamics, that is broken in active systems. It is, therefore, natural that field theories that aim

to describe the behaviour of active matter have to revisit the foundations and need to go beyond the detailed-balance restrictions. Successive works culminated in the recently introduced, so-called *Active Model B+ (AMB+)* [53–55], that attracted a lot of interest lately [56–59]. Continuum approaches, very recently, have also been extended to include active chirality and specifically account for broken-time reversal symmetries [36, 60, 61].

The modelling of inter-particle interactions is crucial for such continuum approaches. While previous approaches are predominantly focused on interaction potentials, here we model the interactions via a geometric approach instead. The approach was originally introduced by Bruna and Chapman in [62, 63] and thereafter successfully applied to ABPs already [64]. The basic idea is to include particle interactions by restricting the domain of definition of the time-evolution equation and thereby creating forbidden areas, which correspond to situations with a particle overlap. We apply this idea to the ACP model and derive an effective one-body description of the full one-particle PDF $p(\mathbf{x}, \theta, t)$ to find a particle at position $\mathbf{x}$ with the self-propulsion vector of angle θ at time t after starting with the sharp initial conditions $\mathbf{x} = \mathbf{x}_0$, $\theta = \theta_0$, i.e. $p(\mathbf{x}, \theta, t_0) = \delta(\mathbf{x} - \mathbf{x}_0)\,\delta(\theta - \theta_0)$ at $t = t_0$. The resulting time-evolution equation explicitly accounts for two-particle steric interactions and therefore its validity is restricted to the dilute limit. To arrive at a field-theoretical description for the mean particle PDF $\varrho(\mathbf{x}, t)$, one typically proceeds by integrating out the effect of the angle [65, 66]. We follow this procedure and arrive at an (infinite) hierarchy of the hydrodynamic modes of the active particle, of which the mean particle PDF constitutes the zeroth order mode. This hierarchy is mathematically very similar to the famed Bogoliubov–Born–Green–Kirkwood–Yvon (BBGKY) hierarchy in kinetic theory [67]. Similar to that hierarchy, in continuous active matter theories one is also required to close the hierarchy to make analytic progress [68, 69].

We transform the closure problem into a perturbation problem and derive two field-theoretical descriptions for ACPs, based on the strictness of assumption on the perturbation parameters. This gives us access to the otherwise phenomenological coefficients in these models. We show that both an effective diffusive description and the AMB+ can be obtained within our approach, depending on the order of the closure scheme. Our work moreover suggests that the AMB+ is a natural generalisation of equilibrium field theories to describe the continuum behaviour of active matter. We further have first-principles access to the coefficients in the AMB+ and it turns out, that, surprisingly, they are altered by active chirality in such a way that they can even change sign as a function of chirality.

The remainder of this work is organised as follows. In section 2.1 we introduce the mathematical model and describe our approach to deal with inter-particle interactions in the geometric sense. In section 2.2 we derive in detail the effective one-body time-evolution equation of the PDF. To our understanding, the physics community is rather unaware of this specific method to handle inter-particle interactions, for which we introduce it in appropriate detail. In section 2.3 we thereafter derive the hierarchy of hydrodynamic modes, and in section 2.4 we introduce the mathematical steps to close the hierarchy. In section 2.5 we go one step beyond the simplest closure and find that the time-evolution of the mean particle PDF equals the form predicted by the AMB+. In section 3 we conclude and provide an outlook to further and related works.

2. Theory: from ACPs to the Active Model B $+$

2.1. Model

In this section, we introduce the model of interacting ACPs as sketched in figure 1(a) and how to deal with their excluded-volume interactions in a geometric sense, see also figure 1(b). We finish by formulating an effective one-body description.
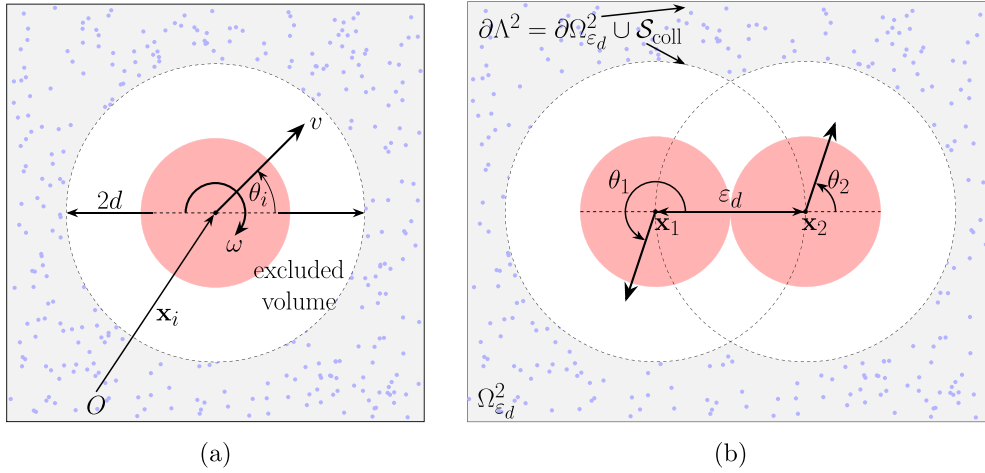
Figure 1. (a) Sketch of the model setup of the *i*th spherical ACP of diameter *d*. The particle is self-propelled by the active speed *v* whose direction rotates with the active frequency ω. It is embedded in a thermal bath giving rise to fluctuations in the spatial and angular coordinates $(\mathbf{x}_i, \theta_i)$ with respective strengths $\propto \sqrt{D_T}$ and $\propto \sqrt{D_R}$, see equations (1*a*) and (1*b*), respectively. (b) The particle coordinates are defined on $\Lambda^2 = \Omega_{\varepsilon_d}^2 \times [0, 2\pi)^2$, where $\Omega_{\varepsilon_d}^2 = \{(\mathbf{x}_1, \mathbf{x}_2) \in \Omega^2; |\mathbf{x}_1(t) - \mathbf{x}_2(t)| \geqslant \varepsilon_d\}$ is the allowed (rescaled) configuration space within the bounded domain $\Omega \subset \mathbb{R}^2$ and subtracted by the regions of a particle overlap (white area). This excluded-volume creates a reflecting boundary on $\partial \Lambda^2 = \partial \Omega^2 \cup \mathcal{S}_{\text{coll}}$, made up from the container walls $\partial \Omega^2$ and an inner moving, so-called collision surface $\mathcal{S}_{\text{coll}} = \{(\mathbf{x}_1, \mathbf{x}_2) \in \Omega^2; |\mathbf{x}_1(t) - \mathbf{x}_2(t)| = \varepsilon_d\}$. Note that $\varepsilon_d = d/L$, where $L \times L = |\Omega|$ is the typical size of the bounded domain Ω.

2.1.1. Setup. We consider the dynamics of *N* interacting ACPs in two dimensions. The particles centres $\mathbf{x}_i(t)$ and angular coordinates $\theta_i(t)$, $i \in \{1, \dots, N\}$ move according to the overdamped Langevin dynamics [5, 70]

$$\frac{\partial}{\partial t} \mathbf{x}_i = v \hat{\mathbf{e}}(\theta_i) + \sqrt{2D_T}\, \boldsymbol{\eta}_i(t), \tag{1a}$$

$$\frac{\partial}{\partial t} \theta_i = \omega + \sqrt{2D_R}\, \zeta_i(t). \tag{1b}$$

Here $\boldsymbol{\eta}_i(t)$ and $\zeta_i(t)$ are independent Gaussian white noises with correlators $\langle \eta_{i,\alpha}(t) \eta_{j,\beta}(t') \rangle = \delta_{ij} \delta_{\alpha\beta} \delta(t - t')$ and $\langle \zeta_i(t) \zeta_j(t') \rangle = \delta_{ij} \delta(t - t')$, where Greek indices α, β refer to particle coordinates and Latin indices i, j refer to particle labels. *v* is the (constant) active self-propulsion velocity, ω the active torque and $\hat{\mathbf{e}}(\theta_i) = (\cos(\theta_i), \sin(\theta_i))^T$ is the unit orientation vector, where $(\cdot)^T$ denotes a matrix transpose. Note that for $\omega = 0$, the model of equations (1*a*) and (1*b*) reduces to the well-known model of ABPs. D_T and D_R are the translational and rotational diffusion coefficients, respectively. Note that the diffusion coefficients have different physical units, $[D_T] = m^2/s$ and $[D_R] = 1/s$.

The *N* identical disk-like particles have a diameter *d* and are assumed to interact hard-core with each other. For an illustration of the model system see also figure 1(a). The ACPs are modelled to diffuse in a spatially bounded domain $\mathbf{x}_i(t) \in \Omega \subset \mathbb{R}^2$ of typical size $L \times L$ and their angular coordinates are $\theta_i(t) \in [0, 2\pi)$. Using dimensionless quantities by rescaling with *L*, the typical size of the domain is set to unity, whereas the diameter of the particle becomes

$\varepsilon_d = d/L$. We restrict the analysis to a dilute system, i.e. we assume that $N\varepsilon_d \ll 1$. In contrast to typical approaches to model the interactions, that is, via an interaction-potential term in the spatial Langevin equation (1*a*), we instead restrict the domain of definition of the centre-of-mass coordinates $\mathbf{x}_i(t)$. We thereby follow a geometric approach to model particle interactions as established by Bruna and Chapman [62, 63] that already has proven successful in various contexts [71–73]. These authors also showed in a recent work [64] that within this model they can derive additional nonlinear cross-diffusion terms for the description of sterically interacting ABPs, compared to more classical treatments of interacting ABPs [74, 75].

The fundamental idea in modelling steric interactions in this geometric sense is that equation (1*a*) is defined on a restricted (spatial) domain $\Omega_{\varepsilon_d}^N = \{(\mathbf{x}_1,\ldots,\mathbf{x}_N) \in \Omega^N; \forall i \neq j : |\mathbf{x}_i(t) - \mathbf{x}_j(t)| \geqslant \varepsilon_d\}$ due to the excluded volume. The full model including equation (1*b*) therefore is defined on $\Lambda^N = \Omega_{\varepsilon_d}^N \times [0, 2\pi)^N$. Note that as the angular coordinate is not affected by the steric interactions, its domain of definition is not restricted. While for the angular coordinate we assume periodic boundary conditions, the cost of treating the particle interactions by restricting the domain of definition is that we have generated an inner (moving) boundary as apparent from figure 1(a). At this boundary, particles perform hard elastic collisions similar to the container walls. Both inner and container-wall boundaries therefore are treated with reflective boundaries. To simplify this problem, we observe that for a dilute system finding configurations in the system where three particles are close, or two particles are close to a container wall is of the order $\mathcal{O}(\varepsilon_d^2 N^2)$. Configurations where two particles are close or one particle is close to the wall, in contrast, are of the order $\mathcal{O}(\varepsilon_d N)$ [62, 63]. It is therefore reasonable to assume that in a dilute system, two-body collisions dominate the interactions and we can safely ignore higher-order correlations. As we assume that all particles are identical, it is sufficient to consider a system with $N = 2$ particles. In the end we will scale the resulting interaction contribution by the particle number, which is justified as long as we stay within the dilute limit.

2.1.2. Joint Fokker–Planck equation.   The Fokker-Planck equation (FPE) for the two-body joint PDF $P_2(t) = P_2(\mathbf{x}_1, \theta_1, \mathbf{x}_2, \theta_2, t)$, defined on Λ^2, reads [76]

$$\frac{\partial}{\partial t} P_2(t) = \nabla_1 \cdot [D_{\mathrm{T}}\nabla_1 - v\hat{\mathbf{e}}(\theta_1)] P_2(t) + \frac{\partial}{\partial \theta_1}\left[D_{\mathrm{R}}\frac{\partial}{\partial \theta_1} - \omega\right] P_2(t)$$
$$+ \nabla_2 \cdot [D_{\mathrm{T}}\nabla_2 - v\hat{\mathbf{e}}(\theta_2)] P_2(t) + \frac{\partial}{\partial \theta_2}\left[D_{\mathrm{R}}\frac{\partial}{\partial \theta_2} - \omega\right] P_2(t). \qquad (2a)$$

Here ∇_i denotes the partial differential vector operator with respect to the position of particle $i \in \{1,2\}$. The reflective boundary condition reads

$$\mathbf{n}_1 \cdot [D_{\mathrm{T}}\nabla_1 - v\hat{\mathbf{e}}(\theta_1)] P_2(t) + \mathbf{n}_2 \cdot [D_{\mathrm{T}}\nabla_2 - v\hat{\mathbf{e}}(\theta_2)] P_2(t) = 0, \qquad (2b)$$

valid on $\partial\Lambda^2 = \partial\Omega_{\varepsilon_d}^2 = \partial\Omega^2 \cup \mathcal{S}_{\mathrm{coll}}$, where $\mathcal{S}_{\mathrm{coll}} = \{(\mathbf{x}_1, \mathbf{x}_2) \in \Omega^2; |\mathbf{x}_1(t) - \mathbf{x}_2(t)| = \varepsilon_d\}$ is the so-called (inner) *collision surface*. For an illustration see figure 1(b). $\mathbf{n}_i$ in equation (2*b*) is the outward unit normal vector of disk i. Note that $\mathbf{n}_i = 0$ for $\mathbf{x}_j \in \partial\Omega^2$ for $(i,j) = (1,2)$ and $(2,1)$ due to particle conservation, as well as $\mathbf{n}_1 = -\mathbf{n}_2$ on $\mathcal{S}_{\mathrm{coll}}$, due to elastic collisions of particles. For the angular coordinate equation (2*a*) is supplemented with the periodic boundary condition

$$P_2(\theta_i = 0) = P_2(\theta_i = 2\pi). \qquad (2c)$$

It is convenient to use the structural similarities of the spatial and angular coordinates and write equation (2*a*) in terms of joint variables $\chi_i = (\mathbf{x}_i, \theta_i)$. The diffusion coefficients form

a diffusion matrix $\mathbf{D} = \mathrm{diag}(D_\mathrm{T}, D_\mathrm{T}, D_\mathrm{R})$ and the joint drift reads $\mathbf{f}(\theta_i) = (v\hat{\mathbf{e}}(\theta_i), \omega)^\mathrm{T}$. The FPE (2*a*) written in the joint variables becomes

$$\frac{\partial}{\partial t} P_2(t) = \nabla_{\chi_1} \cdot [\mathbf{D}\nabla_{\chi_1} - \mathbf{f}(\theta_1)] P_2(t) + \nabla_{\chi_2} \cdot [\mathbf{D}\nabla_{\chi_2} - \mathbf{f}(\theta_2)] P_2(t), \qquad (3)$$

valid on Λ^2. We here use the joint partial differential operator $\nabla_{\chi_i} = (\nabla_i, \partial/\partial\theta_i)^\mathrm{T}$.

We are interested in analytically capturing the effects of particle collisions on the one-body diffusive behaviour. Therefore, we aim at deriving an effective description for the full one-body PDF $p(\mathbf{x}_1, \theta_1, t) = p(\chi_1, t)$, which is defined as

$$p(\chi_1, t) = \int_{\Lambda(\chi_1)} \mathrm{d}\chi_2 \, P_2(t) = \int_0^{2\pi} \mathrm{d}\theta_2 \int_{\Omega \backslash \mathrm{B}_{\varepsilon_d}(\mathbf{x}_1)} \mathrm{d}\mathbf{x}_2 \, P_2(t), \qquad (4)$$

where we take particle one to be the test particle of interest. The area $\Lambda(\chi_1)$ of integration is given by all allowed configurations for the second particle to be placed everywhere apart from the excluded volume created by the first particle, i.e. $\Lambda(\chi_1) = \Omega \backslash \mathrm{B}_{\varepsilon_d}(\mathbf{x}_1) \times [0, 2\pi)$, where $\mathrm{B}_{\varepsilon_d}(\mathbf{x}_1)$ is the disk of radius ε_d centred at $\mathbf{x}_1$.

2.2. Effective one-body description

In this section, we perform the integration to arrive at an effective one-body description and encounter that the effect of particle collisions results in a so-called collision integral. We solve this integral by the method of matched asymptotic expansions and provide the effective one-body description. This section follows [64] and adapts it to ACPs to review and introduce the geometric method to deal with particle interactions to the reader.

2.2.1. The collision integral. Integrating equation (2*a*) over the reduced configuration space $\Lambda(\chi_1)$ results in

$$\frac{\partial}{\partial t} p(\chi_1, t) = \int_{\Lambda(\chi_1)} \mathrm{d}\chi_2 \, \nabla_{\chi_1} \cdot [\mathbf{D}\nabla_{\chi_1} - \mathbf{f}(\theta_1)] P_2(t)$$
$$+ \int_{\Lambda(\chi_1)} \mathrm{d}\chi_2 \, \nabla_{\chi_2} \cdot [\mathbf{D}\nabla_{\chi_2} - \mathbf{f}(\theta_2)] P_2(t). \qquad (5)$$

We can easily evaluate the second integral, in which integration and differentiation are with respect to the same variable. Using the divergence theorem and applying the boundary conditions of equations (2*b*) and (2*c*), we find

$$\int_{\Lambda(\chi_1)} \mathrm{d}\chi_2 \, \nabla_{\chi_2} \cdot [\mathbf{D}\nabla_{\chi_2} - \mathbf{f}(\theta_2)] P_2(t)$$
$$= \int_0^{2\pi} \mathrm{d}\theta_2 \int_{\partial \mathrm{B}_{\varepsilon_d}(\mathbf{x}_1)} \mathrm{dS}_2 \, \mathbf{n}_2 \cdot [D_\mathrm{T}\nabla_1 - v\hat{\mathbf{e}}(\theta_1)] P_2(t), \qquad (6)$$

where $\mathrm{dS}_2 \, \mathbf{n}_2$ is the outward surface element of $\mathbf{x}_2$ and we used that $\mathbf{n}_1 = -\mathbf{n}_2$ on $\partial \mathrm{B}_{\varepsilon_d}(\mathbf{x}_1)$ and $\mathbf{n}_1 = 0$ for $\mathbf{x}_2 \in \partial\Omega$.

The first integral in equation (5) cannot be evaluated that simply since integration and differentiation are with respect to different particle labels. Instead, we have to use the Reynolds

transport theorem extended to spatial variation of integrals [77, 78]. Together with an additional use of the divergence theorem this results in

$$
\int_{\Lambda(\chi_1)} \mathrm{d}\chi_2 \, \nabla_{\chi_1} \cdot [\mathbf{D}\nabla_{\chi_1} - \mathbf{f}(\theta_1)] P_2(t) = \nabla_{\chi_1} \cdot [\mathbf{D}\nabla_{\chi_1} - \mathbf{f}(\theta_1)] p(\chi_1, t)
$$
$$
- \int_0^{2\pi} \mathrm{d}\theta_2 \int_{\partial \mathrm{B}_{\varepsilon_d}(\mathbf{x}_1)} \mathrm{d}\mathrm{S}_2 \, \mathbf{n}_2 \cdot [D_{\mathrm{T}}(2\nabla_1 + \nabla_2) + v\hat{\mathbf{e}}(\theta_1)] P_2(t). \tag{7}
$$

For details of this calculation, see the appendix. We combine this integral with equation (6) and find the effective equation for the full one-body PDF $p(\chi_1, t)$ according to equation (5) as

$$
\frac{\partial}{\partial t} p(\chi_1, t) = \nabla_{\chi_1} \cdot [\mathbf{D}\nabla_{\chi_1} - \mathbf{f}(\theta_1)] p(\chi_1, t)
$$
$$
- D_{\mathrm{T}} \int_0^{2\pi} \mathrm{d}\theta_2 \int_{\partial \mathrm{B}_{\varepsilon_d}(\mathbf{x}_1)} \mathrm{d}\mathrm{S}_2 \, \mathbf{n}_2 \cdot (\nabla_1 + \nabla_2) P_2(\chi_1, \chi_2, t). \tag{8}
$$

In analogy to kinetic theory [67], we refer to this integral as the *collision integral* and denote it by $I(\chi_1, t)$. It captures the effect of two-body hard-disk collisions on a probabilistic level. To evaluate this integral, we have to find an expression for the joint PDF $P_2(\chi_1, \chi_2, t)$ in terms of the one-body PDF $p(\chi_1, t)$, similar to the classical closure problem in kinetic theory, known as the BBGKY hierarchy. This relation will be specifically relevant in regions where the particles are close, and where evaluating the collision integral will contribute to the effective description.

2.2.2. Matched asymptotic expansion.　　We aim at an approximation for P_2 via the method of matched asymptotic expansion [62–64, 71, 79]. We can suppose that when the particles are far apart they are independent, given the hard-disk nature of the interaction. In this so-called *outer region*, we define the *outer joint PDF* as $P^{\mathrm{out}}(\chi_1, \chi_2, t) = P_2(\chi_1, \chi_2, t)$ and due to the independence argument we find that

$$
P^{\mathrm{out}}(\chi_1, \chi_2, t) = p(\chi_1, t) \, p(\chi_2, t) + \varepsilon_d P^{\mathrm{out}}_{(1)}(\chi_1, \chi_2, t) + \mathcal{O}(\varepsilon_d^2). \tag{9}
$$

Note that $P^{\mathrm{out}}_{(1)}$ is a function denoting the corrections at first order $\mathcal{O}(\varepsilon_d)$ to the independence argument [80].

In contrast, when the two particles are close, the particles are correlated due to interactions and we perform a variable change in this so-called *inner region*. We fix particle one and measure the distance to this particle with respect to ε_d, see figure 2. The coordinate change reads as $(\chi_1, \mathbf{x}_2, \theta_2) \mapsto (\chi_1, \mathbf{x}_1 + \varepsilon_d \mathbf{x}, \theta_1 + \theta)$. The *inner PDF* is defined as $P^{\mathrm{in}}(\chi_1, \mathbf{x}, \theta, t) = P_2(\chi_1, \chi_2, t)$. Rewriting the two-particle problem into inner coordinates, we find

$$
\varepsilon_d^2 \frac{\partial}{\partial t} P^{\mathrm{in}} = 2D_{\mathrm{T}} \nabla_{\mathbf{x}}^2 P^{\mathrm{in}} + \varepsilon_d \nabla_{\mathbf{x}} \cdot [v(\hat{\mathbf{e}}(\theta_1) - \hat{\mathbf{e}}(\theta_1 + \theta)) - 2D_{\mathrm{T}} \nabla_{\mathbf{x}_1}] P^{\mathrm{in}}
$$
$$
+ \varepsilon_d^2 \nabla_{\mathbf{x}} \cdot [D_{\mathrm{T}} \nabla_{\mathbf{x}} - v\hat{\mathbf{e}}(\theta_1)] P^{\mathrm{in}} + \varepsilon_d^2 \left[D_{\mathrm{R}} \left(\frac{\partial}{\partial \theta_1} - \frac{\partial}{\partial \theta} \right)^2 - \omega \frac{\partial}{\partial \theta_1} \right] P^{\mathrm{in}}. \tag{10a}
$$

The no-flux boundary condition then translates into inner coordinates as

$$
2D_{\mathrm{T}} \mathbf{x} \cdot \nabla_{\mathbf{x}} P^{\mathrm{in}} = \varepsilon_d \mathbf{x} \cdot [D_{\mathrm{T}} \nabla_{\mathbf{x}_1} - v(\hat{\mathbf{e}}(\theta_1) - \hat{\mathbf{e}}(\theta_1 + \theta))] P^{\mathrm{in}}, \tag{10b}
$$

which is valid on the collision surface $\mathcal{S}_{\mathrm{coll}}$ defined in inner coordinates by $\{\mathbf{x} \in \mathbb{R}^2; |\mathbf{x}| = 1\}$. When formulating the problem in inner coordinates, we have an additional boundary condition,
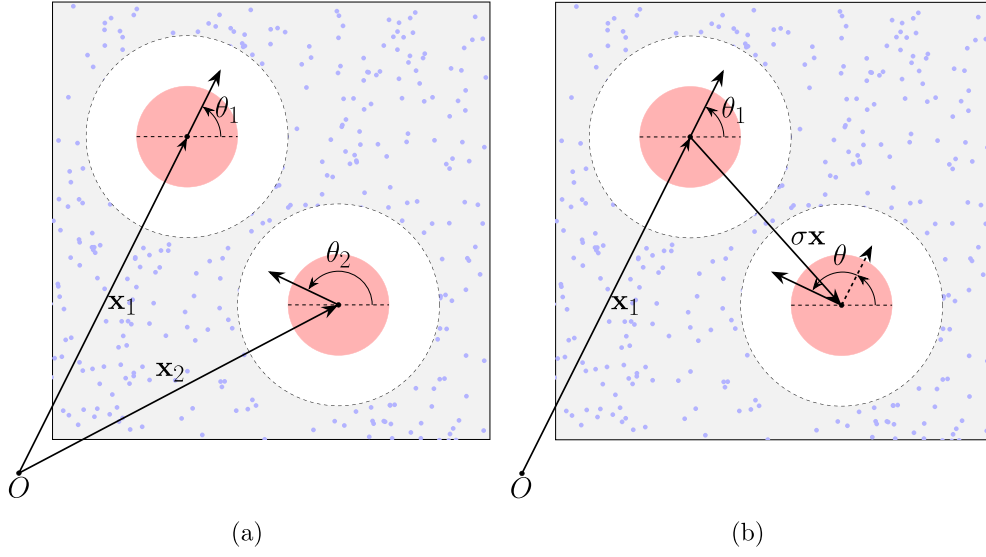
Figure 2. The description of the problem changes from a particle-focused to a fixed-particle perspective. The second particle is measured in relative units. Technically we change from a description of $(\mathbf{x}_1, \theta_1)$ for particle one and $(\mathbf{x}_2, \theta_2)$ for particle two in (a) to a description of $(\mathbf{x}_1, \theta_1)$ for the effectively fixed particle one and the relative coordinate $(\mathbf{x}_1 + \varepsilon_d \mathbf{x}, \theta_1 + \theta)$ for particle two in (b). One advantage of this coordinate change is that the collision surface in the new coordinates is given by the condition $|\mathbf{x}| = 1$.

which is replacing the otherwise implicit natural boundary condition on P_2, i.e. $\lim_{|\mathbf{x}_i| \to \infty} P_2 = 0, i \in \{1, 2\}$. In the framework of the matched asymptotic expansion, this condition implies that the inner PDF has to match the outer PDF as $|\mathbf{x}| \to \infty$. An expansion of the outer solution in inner coordinates gives

$$P^{\text{out}}(\chi_1, \chi_2, t) = p\, p^+ + \varepsilon_d \left(p\, \mathbf{x} \cdot \nabla_{\mathbf{x}_1} p^+ + P_{(1)}^{\text{out},+} \right) + \mathcal{O}\left(\varepsilon_d^2\right), \tag{10c}$$

where we have introduced the shorthand notations $p = p(\chi_1, t)$, $p^+ = p(\mathbf{x}_1, \theta_1 + \theta, t)$ and $P_{(1)}^{\text{out},+} = P_{(1)}^{\text{out}}(\chi_1, \mathbf{x}_1, \theta_1 + \theta, t)$ [64]. Expanding the inner solution in powers of ε_d, $P^{\text{in}} = P_{(0)}^{\text{in}} + \varepsilon_d P_{(1)}^{\text{in}} + \mathcal{O}(\varepsilon_d^2)$, the zeroth-order inner problem becomes

$$0 = 2D_{\text{T}}\, \nabla_{\mathbf{x}}^2 P_{(0)}^{\text{in}}, \tag{11a}$$

$$0 = 2D_{\text{T}}\, \mathbf{x} \cdot \nabla_{\mathbf{x}} P_{(0)}^{\text{in}}, \qquad \text{on } |\mathbf{x}| = 1, \tag{11b}$$

$$P_{(0)}^{\text{in}} \sim p p^+, \qquad \text{as } |\mathbf{x}| \to \infty, \tag{11c}$$

with the straight-forward solution

$$P_{(0)}^{\text{in}} = p p^+. \tag{12}$$

Note here, that $P_{(0)}^{\text{in}}$ is no function of the separation coordinate $\mathbf{x}$.

Before we can write the first-order inner problem, we note from equation (10a), that at order $\mathcal{O}(\varepsilon_d)$, we have that

$$0 = 2D_{\text{T}}\, \nabla_{\mathbf{x}}^2 P_{(1)}^{\text{in}} + \varepsilon_d \nabla_{\mathbf{x}} \cdot \left[v\left(\hat{\mathbf{e}}(\theta_1) - \hat{\mathbf{e}}(\theta_1 + \theta) \right) - 2D_{\text{T}}\, \nabla_{\mathbf{x}_1} \right] P_{(0)}^{\text{in}}$$

$$= 2D_{\text{T}}\, \nabla_{\mathbf{x}}^2 P_{(1)}^{\text{in}}, \tag{13}$$

8

as $P_{(0)}^{\text{in}}$ is no function of the separation variable $\mathbf{x}$. Taking this into account, the first-order inner problem reads

$$0 = 2D_{\text{T}} \, \nabla_{\mathbf{x}}^2 P_{(1)}^{\text{in}}, \tag{14a}$$

$$\mathbf{x} \cdot \nabla_{\mathbf{x}} P_{(1)}^{\text{in}} = \mathbf{x} \cdot \mathbf{A}\left(\chi_1, \theta, t\right), \qquad \text{on } |\mathbf{x}| = 1, \tag{14b}$$

$$P_{(1)}^{\text{in}} \sim \mathbf{x} \cdot \mathbf{B}\left(\chi_1, \theta, t\right) + P_{(1)}^{\text{out},+}, \qquad \text{as } |\mathbf{x}| \to \infty, \tag{14c}$$

where

$$\mathbf{A}\left(\chi_1, \theta, t\right) = \frac{1}{2D_{\text{T}}} \left(D_{\text{T}} \, \nabla_{\mathbf{x}_1}\left(pp^+\right) - v\left(\hat{\mathbf{e}}\left(\theta_1\right) - \hat{\mathbf{e}}\left(\theta_1 + \theta\right)\right)pp^+\right), \tag{15}$$

$$\mathbf{B}\left(\chi_1, \theta, t\right) = p \, \nabla_{\mathbf{x}_1}p^+. \tag{16}$$

The solution can be obtained straightforwardly and is given by [62, 63, 73, 77]

$$P_{(1)}^{\text{in}} = a + P_{(1)}^{\text{out},+} + \mathbf{x} \cdot \mathbf{B} - \frac{\mathbf{x}}{|\mathbf{x}|^2} \cdot (\mathbf{A} - \mathbf{B}), \tag{17}$$

where a is an arbitrary integration constant. According to the expansion ansatz $P^{\text{in}} \sim P_{(0)}^{\text{in}} + \varepsilon_d P_{(1)}^{\text{in}} + \mathcal{O}(\varepsilon_d^2)$ for the inner PDF, we thus found that

$$P^{\text{in}} = pp^+ + \varepsilon_d \mathbf{x} \cdot p \, \nabla_{\mathbf{x}_1}p^+ - \varepsilon_d \frac{\mathbf{x}}{2|\mathbf{x}|^2} \cdot \left[p^+ \, \nabla_{\mathbf{x}_1}p - p \, \nabla_{\mathbf{x}_1}p^+ \right.$$
$$\left. - \frac{v}{D_{\text{T}}} \left(\hat{\mathbf{e}}\left(\theta_1\right) - \hat{\mathbf{e}}\left(\theta_1 + \theta\right)\right)pp^+\right] + \varepsilon_d\left(a + P_{(1)}^{\text{out},+}\right) + \mathcal{O}\left(\varepsilon_d^2\right). \tag{18}$$

2.2.3. Evaluation of the collision integral. We now use this approximate inner solution to evaluate the collision integral. In inner coordinates, this is given by

$$I(\chi_1, t) = \varepsilon_d D_{\text{T}} \int_0^{2\pi} \mathrm{d}\theta \int_{|\mathbf{x}|=1} \mathrm{d}S_{\mathbf{x}} \, \mathbf{x} \cdot \nabla_{\mathbf{x}_1} P^{\text{in}}\left(\chi_1, \mathbf{x}, \theta, t\right), \tag{19}$$

where we used that $\mathbf{n}_{\mathbf{x}} = -\mathbf{x}$ on the collision surface $\mathcal{S}_{\text{coll}}$. Using the inner solution of equation (18), the collision integral becomes

$$I(\chi_1, t) = \varepsilon_d D_{\text{T}} \int_0^{2\pi} \mathrm{d}\theta \left[\nabla_{\mathbf{x}_1}\left(pp^+\right)\right]_\alpha \int_{|\mathbf{x}|=1} \mathrm{d}S_{\mathbf{x}} \, x_\alpha$$
$$+ \varepsilon_d^2 D_{\text{T}} \int_0^{2\pi} \mathrm{d}\theta \left[\nabla_{\mathbf{x}_1} P_{(1)}^{\text{out},+}\right]_\alpha \int_{|\mathbf{x}|=1} \mathrm{d}S_{\mathbf{x}} \, x_\alpha$$
$$+ \varepsilon_d^2 D_{\text{T}} \int_0^{2\pi} \mathrm{d}\theta \left[\nabla_{\mathbf{x}_1}\left(p\nabla_{\mathbf{x}_1}p^+\right)_\alpha\right]_\beta \int_{|\mathbf{x}|=1} \mathrm{d}S_{\mathbf{x}} \, x_\alpha x_\beta$$
$$- \varepsilon_d^2 \frac{D_{\text{T}}}{2} \int_0^{2\pi} \mathrm{d}\theta \left[\nabla_{\mathbf{x}_1}\left(p^+ \, \nabla_{\mathbf{x}_1}p - p \, \nabla_{\mathbf{x}_1}p^+\right)_\alpha\right]_\beta \int_{|\mathbf{x}|=1} \mathrm{d}S_{\mathbf{x}} \, \frac{x_\alpha x_\beta}{|\mathbf{x}|^2}$$
$$- \varepsilon_d^2 \frac{v}{2} \int_0^{2\pi} \mathrm{d}\theta \left[\hat{\mathbf{e}}\left(\theta_1\right) - \hat{\mathbf{e}}\left(\theta_1 + \theta\right)\right]_\alpha \left[\nabla_{\mathbf{x}_1}\left(pp^+\right)\right]_\beta \int_{|\mathbf{x}|=1} \mathrm{d}S_{\mathbf{x}} \, \frac{x_\alpha x_\beta}{|\mathbf{x}|^2} \tag{20}$$

where we introduced the Einstein convention, i.e. that the sum over double indices is implicit: $x_\alpha x_\alpha = \sum_{\alpha=1}^2 x_\alpha x_\alpha$. There are two types of integrals appearing in equation (20), namely, an integral of an outer unit normal vector over the whole unit sphere: $\int_{|\mathbf{x}|=1} \mathrm{dS}_\mathbf{x}\, x_\alpha = 0$, by geometrical insight; and

$$\int_{|\mathbf{x}|=1} \mathrm{dS}_\mathbf{x}\, \frac{x_\alpha x_\beta}{|\mathbf{x}|^2} = \int_{|\mathbf{x}|=1} \mathrm{dS}_\mathbf{x}\, x_\alpha x_\beta = \pi\, \delta_{\alpha\beta}, \qquad (21)$$

valid in two dimensions.

As θ_1 is independent of θ and kept constant for the variation of θ, we can define a new variable $\tilde\theta = \theta_1 + \theta$ and use it to integrate out the θ-dependence in equation (20). Therefore, we define the *mean particle PDF*

$$\varrho(\mathbf{x},t) = \int_0^{2\pi} \mathrm{d}\tilde\theta\, p(\mathbf{x},\tilde\theta,t), \qquad (22)$$

and the *polarisation*

$$\boldsymbol{\sigma}(\mathbf{x},t) = 2\int_0^{2\pi} \mathrm{d}\tilde\theta\, p(\mathbf{x},\tilde\theta,t)\, \hat{\mathbf{e}}(\tilde\theta), \qquad (23)$$

as the zeroth and first-order moment of the full one-body PDF, respectively. Note the factor of 2 in the definition of the polarisation, which is necessary for consistency later on. Thus, the collision integral becomes

$$I(\chi_1,t) = \varepsilon_d^2 \frac{\pi}{2}\, \nabla_{\mathbf{x}_1} \cdot \left[3D_\mathrm{T} p\, \nabla_{\mathbf{x}_1}\varrho - D_\mathrm{T}\varrho\, \nabla_{\mathbf{x}_1}p + v\left(\hat{\mathbf{e}}(\theta_1)\varrho - \frac{\boldsymbol{\sigma}}{2}\right)p \right], \qquad (24)$$

where $\varrho = \varrho(\mathbf{x}_1,t)$, $\boldsymbol{\sigma} = \boldsymbol{\sigma}(\mathbf{x}_1,t)$, and, as a reminder, $p = p(\mathbf{x}_1,\theta_1,t)$.

As expected, the dependence on the separation coordinates $\mathbf{x}$ and θ vanished, since we integrated out the effect of the second particle on the first. Thus, we can back-transform into the original variables and then drop the index in the notation $(\mathbf{x}_1,\theta_1) \mapsto (\mathbf{x},\theta)$, similarly for the operator $\nabla_1 \mapsto \nabla$. We insert the evaluated collision integral into equation (8) and find the effective time-evolution equation for the full one-body PDF p. This equation is valid for two hard-interacting particles. As introduced in the beginning, in the dilute system of N particles, we can safely assume that two-particle collisions dominate any higher-order correlations. The tagged particle can have $(N-1)$ inner regions with each of the remaining particles under this assumption. It is thus sufficient to multiply the collision integral by the factor of $(N-1)$ to account for the interaction effect in the effective, dilute one-body description.

2.2.4. Effective one-body equation.　　We introduce the dimensionless parameter $\phi = \varepsilon_d^2 \pi (N-1)/4$, which for large N approximately equals the area fraction of the particles. We then write the obtained time-evolution equation for the full one-body PDF $p = p(\mathbf{x},\theta,t)$ as

$$\frac{\partial}{\partial t}p = -v\, \nabla \cdot [(1-2\phi\varrho)\, \hat{\mathbf{e}} + \phi\boldsymbol{\sigma}]p + \frac{\partial}{\partial\theta}\left[D_\mathrm{R}\frac{\partial}{\partial\theta} - \omega\right]p$$
$$+ D_\mathrm{T}\, \nabla \cdot [(1-2\phi\,\varrho)\, \nabla p + 6\phi p\, \nabla\varrho], \qquad (25)$$

valid in the dilute limit, i.e. $\phi \ll 1$. Without the effect of chirality ($\omega = 0$) this equation was recently derived in [64] for ABPs. When compared with alternative approaches, this systematic derivation of the one-body description results in additional cross-diffusion terms ($\propto \varrho\nabla p$, $\propto p\nabla\varrho$). These terms were not reported in, e.g. literature on phenomenological approaches [74, 75], works relying on approximations of the pair correlation function [57, 81], or classical

dynamical density functional theory [82, 83]. These cross-diffusion terms, however, become specifically important when dealing with different particle labels, and thus accounting for particle-identity in the effective description [62, 73]. Further, recent work shows that for ABPs, equation (25) forms a well-posed problem for which a stationary state exists [84].

In the context of phase-separating active matter, typically effective self-propulsion velocities $v(\varrho)$ are introduced [18, 85] and constitute an essential theoretical trick to observe phase separation in purely repulsive active systems [65]. To the lowest order in density, they are typically of the form of $v(\varrho) = v_0(1 - a\phi\varrho)(v_0 = \text{const})$ which was also derived using linear response theory [86]. The reason is simple: in regions with many particles, the effective swim speed must be reduced. It is interesting that we naturally obtain this form in the geometric integration procedure for hard interactions, and we can constitute that $a = 2$ for steric interactions.

2.3. Hierarchy of hydrodynamic equations

We now project the time-evolution equation for the full one-body PDF $p(\mathbf{x}, \theta, t)$ on its angular modes, where the zeroth-order mode is given by the mean particle PDF $\varrho(\mathbf{x}, t)$. This procedure generates a hierarchy of coupled partial differential equations for the time evolution of the modes. We analyse these equations to provide a footing to systematically close the hierarchy in the next section.

2.3.1. Expansion in harmonic modes. To overcome the angular dependence of the full one-body PDF, we expand the full one-body PDF in eigenfunctions of the rotation operator $\partial^2/\partial\theta^2$ in equation (25). This results in a Fourier expansion, in which modes of order $n \in \mathbb{N}_0$ have eigenvalue $-n^2$ in two dimensions. This expansion can be brought into the form

$$p(\mathbf{x}, \theta, t) = \frac{1}{2\pi}\left(\varrho(\mathbf{x}, t) + \boldsymbol{\sigma}(\mathbf{x}, t) \cdot \hat{\mathbf{e}}(\theta) + \mathbf{Q}(\mathbf{x}, t) : \hat{\mathbf{e}}(\theta) \otimes \hat{\mathbf{e}}(\theta) + \Upsilon(\theta)\right), \quad (26)$$

where $\mathbf{Q} : \hat{\mathbf{e}} \otimes \hat{\mathbf{e}} = Q_{\alpha\beta}\hat{e}_\beta\hat{e}_\alpha$ denotes the full contraction with the outer product $\hat{\mathbf{e}} \otimes \hat{\mathbf{e}}$, and $\Upsilon(\theta)$ refers to higher order modes. Notably, higher order (outer) products of the self-propulsion vector $\hat{\mathbf{e}}(\theta) = (\cos(\theta), \sin(\theta))^{\mathrm{T}}$ naturally appear as modes in this expansion. This expansion is also known as a Cartesian multipole expansion [87] and finds wide use in the theory of liquid crystals [88]. Note that there exists an equivalent approach, as other works in active matter use an angular multipole expansion at this stage [25, 65, 89], where the second mode is replaced by $(\hat{\mathbf{e}}(\theta) \otimes \hat{\mathbf{e}}(\theta) - 1/2)$, where $\mathbf{1}$ denotes the identity tensor. The two expansions are equivalent, as $\mathbf{Q}$ is a traceless object, see below.

The coefficients of the expansion are given by the mean particle PDF $\varrho(\mathbf{x}, t)$ (zeroth-order mode), as defined above in equation (22), the mean polarisation $\boldsymbol{\sigma}(\mathbf{x}, t)$ (first-order mode), as defined above in equation (23), and the mean nematic order tensor (second-order mode), defined as

$$\mathbf{Q}(\mathbf{x}, t) = 4\int_0^{2\pi} \mathrm{d}\theta\, p(\mathbf{x}, \theta, t)\left(\hat{\mathbf{e}}(\theta) \otimes \hat{\mathbf{e}}(\theta) - \frac{1}{2}\right). \quad (27)$$

Note that due to the similarity with hydrodynamic theories, the coefficients are sometimes referred to as *hydrodynamic coefficients*, the hierarchy created by them as a *hydrodynamic hierarchy* [65, 69].

The inner product on the unit-sphere is defined in the standard way as

$$\langle f(\theta), g(\theta)\rangle = \int_0^{2\pi} \mathrm{d}\theta\, f(\theta)\, g(\theta), \quad (28)$$

for two functions f and g. The modes of the Cartesian multipole expansion, $\{\hat{\mathbf{e}}^n; n \in \mathbb{N}_0\}$, form an orthogonal basis with respect to this scalar product. Therefore, we can project the full one-body PDF $p(\mathbf{x}, \theta, t)$ onto the modes and obtain the hydrodynamic coefficients

$$\langle p(\mathbf{x}, \theta, t), 1 \rangle = \varrho(\mathbf{x}, t), \tag{29a}$$

$$\langle p(\mathbf{x}, \theta, t), \hat{\mathbf{e}}(\theta) \rangle = \frac{1}{2}\, \boldsymbol{\sigma}(\mathbf{x}, t), \tag{29b}$$

$$\langle p(\mathbf{x}, \theta, t), \hat{\mathbf{e}}(\theta) \otimes \hat{\mathbf{e}}(\theta) \rangle = \frac{1}{4}\, \mathbf{Q}(\mathbf{x}, t). \tag{29c}$$

2.3.2. Time-evolution of modes. Using the orthogonality of modes, we can project the time-evolution equation for the full one-body PDF, equation (25), on each mode to obtain a time-evolution equation for the corresponding hydrodynamic coefficient. Projecting equation (25) on the zeroth-order mode, we obtain a time-evolution equation of the mean particle PDF ϱ, which is given by

$$\frac{\partial}{\partial t}\varrho(\mathbf{x}, t) = D_{\mathrm{T}}\, \nabla_\alpha \left[(1 + 4\phi\, \varrho(\mathbf{x}, t)) \nabla_\alpha \varrho(\mathbf{x}, t) \right] - \frac{v}{2}\, \nabla_\alpha \sigma_\alpha(\mathbf{x}, t). \tag{30}$$

The mean particle PDF therefore obeys a continuity equation. This is expected on physical grounds as ϱ is a conserved quantity. Specifically, this implies that ϱ is a slow variable, i.e. a density perturbation of scale λ relaxes on a time scale which diverges as $\lambda \to \infty$. This observation will be confronted with the time-evolution equation for the higher modes below. We further observe that the equation for the mean particle PDF needs an explicit input from the polarisation $\boldsymbol{\sigma}$. This coupling is induced by the activity v in the model and persist for all modes, which generates a hierarchy. Formally this hierarchy is similar to the famed BBGKY hierarchy of kinetic theory [67], where also higher order modes implicitly alter the time-evolution of the mode in focus.

Projecting equation (25) onto the first order mode, we obtain a time-evolution equation for the mean polarisation $\boldsymbol{\sigma}$, which is given in component-form by

$$\begin{aligned}
\frac{\partial}{\partial t}\sigma_\alpha(\mathbf{x}, t) = {} & D_{\mathrm{T}}\, \nabla_\beta \left[(1 - 2\phi\, \varrho(\mathbf{x}, t)) \nabla_\beta \sigma_\alpha(\mathbf{x}, t) + 6\phi\, \sigma_\beta(\mathbf{x}, t)\, \nabla_\alpha \varrho(\mathbf{x}, t) \right] \\
& - v\, \nabla_\beta \left[(1 - 2\phi\, \varrho(\mathbf{x}, t)) \left(\frac{Q_{\beta\alpha}(\mathbf{x}, t)}{2} + \varrho(\mathbf{x}, t)\, \delta_{\beta\alpha} \right) \right. \\
& \left. + \phi\, \sigma_\beta(\mathbf{x}, t)\, \sigma_\alpha(\mathbf{x}, t) \right] - D_{\mathrm{R}}\, \Gamma_{\alpha\beta} \sigma_\beta(\mathbf{x}, t). \tag{31}
\end{aligned}$$

Again, we observe that the time-evolution equation for the mean polarisation needs both input from the mean particle density ϱ as well as from the nematic order tensor $\mathbf{Q}$. We further observe that in contrast to the time evolution of the mean particle density the structure of this equation is different. While ϱ obeys a continuity equation, equation (31) has a sink term: $-D_{\mathrm{R}}\, \Gamma_{\alpha\beta} \sigma_\beta(\mathbf{x}, t)$. The polarisation, and as we will see, all higher modes therefore are not conserved quantities, and their dynamics are governed by the associated time scale of the sink term. For the mean polarisation, this time scale is given by $\tau_1 = 1/D_{\mathrm{R}}$ [90, 91].

This fundamental structural difference of the time-evolution equations arises in the θ-term of the parental equation (25) of the hierarchy. While for the polarisation we find that $\hat{\mathbf{e}}$ is the $n = 1$st-order eigenfunction of the rotation operator with eigenvalue $-n^2 = -1$, for the

zeroth-order mode ϱ, the eigenvalue is zero. For the chirality-induced term of equation (25), we observe a similar phenomenon. In the projection procedure, we find that

$$\left\langle \hat{e}_\alpha, \omega \frac{\partial}{\partial \theta} p \right\rangle = \omega \int_0^{2\pi} \mathrm{d}\theta\, \hat{e}_\alpha(\theta)\, \frac{\partial}{\partial \theta} p(\mathrm{x},\theta,t) \tag{32a}$$

$$= \omega \hat{e}_\alpha\, p(\mathrm{x},\theta,t) \Big|_0^{2\pi} - \omega \int_0^{2\pi} \mathrm{d}\theta p(\mathrm{x},\theta,t)\, \frac{\partial}{\partial \theta} \hat{e}_\alpha(\theta) \tag{32b}$$

$$= \varepsilon_{\alpha\beta}\, \omega \int_0^{2\pi} \mathrm{d}\theta\, p(\mathrm{x},\theta,t)\, \hat{e}_\beta(\theta) \tag{32c}$$

$$= \frac{\omega}{2}\, \varepsilon_{\alpha\beta}\, \sigma_\beta(\mathrm{x},t), \tag{32d}$$

where we used that $\partial/\partial\theta\, \hat{e}_\alpha(\theta) = -\varepsilon_{\alpha\beta}\, \hat{e}_\beta(\theta)$ and ε is the Levi-Civita symbol in two dimensions, defined by $\varepsilon_{xx} = \varepsilon_{yy} = 0$ and $\varepsilon_{xy} = -\varepsilon_{yx} = 1$. The boundary term in (32b) vanishes due to periodicity. When we are dealing with the zeroth-order mode, in contrast, the projection $\left\langle 1, \omega \frac{\partial}{\partial\theta} p \right\rangle$, reduces to the boundary term and therefore is zero due to periodicity in θ.

The joint effect of the rotation operator and the active chirality is the origin of the sink term $-D_\mathrm{R}\, \Gamma_{\alpha\beta}\sigma_\beta(\mathrm{x},t)$, where $\mathbf{\Gamma} = (1 + \kappa\varepsilon)$ and $\kappa = \omega/D_\mathrm{R}$ is the associated dimensionless parameter accounting for the effect of chirality. In a more general context, this parameter κ is also referred to as the *oddness* parameter [60, 92–94], since under a reversal of the direction of chirality, $\omega \to -\omega$, κ changes sign and therefore switches the off-diagonal elements of the tensor $\mathbf{\Gamma} \to \mathbf{\Gamma}^\mathrm{T}$.

We find the time-evolution equation for the nematic order tensor from projecting equation (25) on the second order mode $\hat{\mathbf{e}} \otimes \hat{\mathbf{e}}$

$$\begin{aligned}
\frac{\partial}{\partial t} Q_{\alpha\beta}(\mathbf{x},t) &= D_\mathrm{T}\, \nabla_\gamma \left[(1 - 2\phi\, \varrho(\mathbf{x},t))\, \nabla_\gamma Q_{\alpha\beta}(\mathbf{x},t) + 6\phi\, Q_{\alpha\beta}(\mathbf{x},t)\, \nabla_\gamma \varrho(\mathbf{x},t) \right] \\
&\quad - v\, \nabla_\gamma \left[(1 - 2\phi\, \varrho(\mathbf{x},t)) A_{\alpha\beta\gamma\delta}\, \sigma_\delta(\mathbf{x},t) + \phi\, \sigma_\gamma(\mathbf{x},t) Q_{\alpha\beta}(\mathbf{x},t) + \mathcal{O}(\Upsilon) \right] \\
&\quad - 4 D_\mathrm{R}\, \tilde{\Gamma}_{\alpha\gamma} Q_{\gamma\beta}(\mathbf{x},t).
\end{aligned} \tag{33}$$

Here $A_{\alpha\beta\gamma\varepsilon} = (\delta_{\alpha\gamma}\delta_{\beta\varepsilon} + \delta_{\alpha\varepsilon}\delta_{\beta\gamma} - \delta_{\alpha\beta}\delta_{\gamma\varepsilon})/2$ and $\tilde{\mathbf{\Gamma}} = (1 + \kappa\varepsilon/2)$ again accounts for the chirality. The structural similarities of this equation to the polarisation equation are that (*i*) equation (33) couples to neighbouring modes in the hierarchy and to the zeroth order mode ϱ and (*ii*) the relaxation dynamics of the nematic tensor is governed by the time scale $\tau_2 = 1/(4D_\mathrm{R})$ induced by the sink term of equation (33). Again we find that $\mathbf{Q}$, as all higher-order modes, is not conserved. We observe that the relaxation time scale originates in the eigenvalues of the rotation operator, i.e. the relaxation time scale of the nth mode is given by $\tau_n = \tau/n^2 = 1/(n^2 D_\mathrm{R})$, where we denote $\tau = \tau_1 = 1/D_\mathrm{R}$ as the fundamental time scale and $n \geqslant 1$.

In principle, the time-evolution equations for all higher-order modes can be found by the same projection procedure as presented before. This results in an infinite system of coupled time-evolution equations. To get an analytical, meaningful result from this hierarchy, we have to close this hierarchy based on physical arguments about negligible contributions from higher-order modes.

2.4. Closure of the hierarchy

We proceed to introduce the physical arguments to close the hierarchy by neglecting higher-order modes. Therefore, this problem naturally amounts to a perturbative analysis of the hierarchy. As the result of the minimal non-trivial closure scheme, we find an effective diffusion equation for the mean particle density.

2.4.1. Adiabatic approximation.

It would be a formidable task to find a general solution for the *n*th order hierarchical equation and plug this into the $(n-1)$th order equation. By such a procedure, one aims to identify quasi-irrelevant modes for the effect on the time evolution of ϱ. But to our best knowledge, such a procedure has never been successfully applied before for a general order. Instead, it is convenient [5, 25, 57, 66, 69, 95–97] to take advantage of the time scale separation in the system. The dynamics of the polarisation and all higher-order modes are governed by their respective time scale $\tau = \tau_1 = 1/D_\mathrm{R}$ induced by rotational diffusion. τ then reasonably can be assumed to be much smaller than the relaxation time scale of the density, which can be arbitrarily large. Therefore, formally we will investigate the limit of $\tau \to 0$, called *adiabatic* or *quasi-stationarity* approximation, since we adiabatically enslave the behaviour of higher order modes to the mean particle density and assume an instantaneous response to changes.

In some approaches, the adiabatic approximation is also handled differently. Especially in the context of phase separations, the nematic order tensor is assumed to be an adiabatic variable, but the polarisation is treated as a dynamical variable. This appears in active Brownian systems [69, 98, 99], but also in active chiral systems [95, 100]. As explicitly shown there, such an ansatz can qualitatively improve the agreement of the analytical prediction with the numerical data, but it can rarely be treated fully analytically when aiming for the effect of higher-order modes on the relaxation of the mean particle PDF. In related hierarchy-closure problems, nevertheless, an analytic treatment of more than one dynamical variable and a shift of the adiabatic assumption to second order has recently been applied successfully in the framework of dynamical density functional theory [101, 102]. Here many-body correlation functions form an analogous hierarchical problem, but the approach is analytically rather involved and it is not obvious how it can be applied to our situation. We, therefore, restrict our analysis to the basic situation and assume all higher-order modes to be adiabatic.

We will demonstrate the adiabatic approximation for the polarisation equation, but the same arguments hold true for all higher-order modes. Pointing out the essentials, equation (31) can be written as

$$\frac{\partial}{\partial t}\sigma_\alpha + \frac{1}{\tau}\Gamma_{\alpha\beta}\sigma_\beta = f_\alpha\left(\varrho, \boldsymbol{\sigma}, \mathbf{Q}\right), \tag{34}$$

where **f** denotes the leftover gradient-structure terms of equation (31). We can solve this equation formally by

$$\sigma_\alpha\left(\mathbf{x}, t\right) = \mathrm{e}^{-\Gamma_{\alpha\beta}t/\tau}\sigma_\beta\left(\mathbf{x}, 0\right) + \int_0^t \mathrm{d}t' \, \mathrm{e}^{-\Gamma_{\alpha\beta}|t-t'|/\tau} f_\beta\left(\varrho, \boldsymbol{\sigma}, \mathbf{Q}\right), \tag{35}$$

where $\varrho, \boldsymbol{\sigma}$ and $\mathbf{Q}$ have to be evaluated at t' inside the integral. The integrating factor $\mathrm{e}^{-\Gamma_{\alpha\beta}t/\tau}$ is defined as the usual matrix-exponential and can be reformulated as

$$\mathrm{e}^{-\Gamma_{\alpha\beta}t/\tau} = \mathrm{e}^{-t/\tau}\left(\cos\left(\kappa\,\frac{t}{\tau}\right)\delta_{\alpha\beta} - \sin\left(\kappa\,\frac{t}{\tau}\right)\varepsilon_{\alpha\beta}\right), \tag{36}$$

using the anti-symmetry property of $\boldsymbol{\Gamma}$. The active chirality $(\kappa \propto \omega)$ therefore results in oscillations, which decay exponentially on the typical time scale τ. The exponential factor further allows us to write $\int_0^\infty \mathrm{d}t \, \exp(-\Gamma_{\alpha\beta}t/\tau) = \tau\Gamma_{\alpha\beta}^{-1}$, which together with $\lim_{\tau \to 0} \exp(-\Gamma_{\alpha\beta}|t|/\tau) = 0_{\alpha\beta}$ for $|t| > 0$ results in $\lim_{\tau \to 0} \Gamma_{\alpha\gamma} \, \exp(-\Gamma_{\gamma\beta}|t|/\tau) = 2\tau \, \delta_{\alpha\beta}\delta(t)$. Here the factor 2 originates from the integrals taken to be for positive times only. The formal solution of equation (35) evaluated in the limit of $\tau \to 0$ thus reads

$$\lim_{\tau \to 0} \sigma_\alpha(\mathbf{x}, t) = \tau\Gamma_{\alpha\beta}^{-1} f_\beta(\varrho, \boldsymbol{\sigma}, \mathbf{Q}), \tag{37}$$

where now $\varrho, \boldsymbol{\sigma}$ and $\mathbf{Q}$ are functions of t. The corresponding adiabatic approximation for the nematic order tensor similarly reads

$$\lim_{\tau \to 0} Q_{\alpha\beta}(\mathbf{x}, t) = 4\tau\tilde{\Gamma}_{\alpha\gamma}^{-1} \, g_{\gamma\beta}(\varrho, \boldsymbol{\sigma}, \mathbf{Q}, \Upsilon), \tag{38}$$

where $\mathbf{g}$ accounts for the leftover terms of equation (33) and the modes again are evaluated at t.

2.4.2. Closure of the hierarchy via perturbation approach. The adiabatic approximation as such does not suffice to close the hierarchy. The coupling to higher order modes in the hierarchy for each mode enters via the activity-induced term $-v \, \nabla \cdot [(1 - 2\phi \, \varrho) \, \hat{\mathbf{e}}p + 2\phi \, \boldsymbol{\sigma}p]$ from the parental equation (25). This coupling already takes place in interaction-free considerations $(\phi = 0)$, as it specifically arises due to the appearance of the self-propulsion vector and first-order mode $\hat{\mathbf{e}}$. To effectively close the hierarchy we therefore have to argue that higher-order modes can be neglected as compared to lower ones. This consequently turns the closure of the hierarchy into a perturbation problem.

We introduce a dimensionless time via the natural time scale of the system τ and dimensionless space via the mean-particle distance $l_{\mathrm{dist}} = L/\sqrt{\phi}$. The two natural physical length scales in the system are the persistence length $l_{\mathrm{pers}} = v/D_{\mathrm{R}}$ induced by activity and the diffusion length scale $l_{\mathrm{diff}} = \sqrt{D_{\mathrm{T}}/D_{\mathrm{R}}}$ induced by thermal equilibrium fluctuations [64]. We denote the parameters, which arise when comparing the physical length scales with the dimensionless length scale l_{dist} as ε_p and ε_D and observe the following relation between them:

$$\varepsilon_p = \frac{l_{\mathrm{pers}}}{l_{\mathrm{dist}}}, \quad \varepsilon_D = \frac{l_{\mathrm{diff}}}{l_{\mathrm{dist}}}, \quad \text{and} \quad \frac{\varepsilon_p}{\varepsilon_D} = \frac{l_{\mathrm{pers}}}{l_{\mathrm{diff}}} = \frac{v}{\sqrt{D_{\mathrm{T}}D_{\mathrm{R}}}} = \mathrm{Pe}. \tag{39}$$

Here Pe stands for the Péclet number, which measures the relation of activity-induced self-propulsion versus thermally induced displacement.

Here we take ε_p and ε_D to be two independent perturbation parameters. We show that depending on their relation to the Péclet number, different field theoretic descriptions can be obtained. The adiabatic assumption thereby justifies independent small active and passive length scales, since both $l_{\mathrm{pers}} \propto \tau$ and $l_{\mathrm{diff}} \propto \tau$. This treatment is in contrast to previous work, where this subtle point of taking both parameters small and not only their ratio (the Péclet number) was often left implicit or was overlooked.

ε_p and ε_D compare the active and passive physical length scales in the system to the dimensionless length scale, which we choose as the mean particle-particle distance. This is a careful choice, since the other natural length scales in the system, the particle diameter d (which also equals the interaction length scale for hard systems) and the typical box size L were too small and too big, respectively, and already form the small parameter $\phi \propto (d/L)^2$. Together with the assumption of a dilute system, the mean particle-particle distance appears as the correct length scale interpolating between a too-narrow or too-coarse-grained view on the dynamics.

The aforementioned analysis reveals that the coupling to higher-order modes takes place in the activity-induced term at each order. To close the hierarchy, we therefore need to decide up to which order we consider the parameter ε_p. For this work, and referring to what is typical in the literature [25, 57, 66, 69, 95–97], we truncate the hierarchy at order $\mathcal{O}(\varepsilon_p^3)$. We thus ignore contributions from higher modes such as Υ in the nematic equation. Together with the adiabatic assumption equation (33) for the nematic tensor thus becomes

$$Q_{\alpha\beta}(\mathbf{x},t) = \frac{\varepsilon_D}{4} \tilde{\Gamma}_{\alpha\delta}^{-1} \nabla_\gamma \left[(1 - 2\phi\, \varrho(\mathbf{x},t))\, \nabla_\gamma Q_{\delta\beta}(\mathbf{x},t) + 6\phi\, Q_{\delta\beta}(\mathbf{x},t)\, \nabla_\gamma \varrho(\mathbf{x},t) \right]. \quad (40)$$

Equation (40) constitutes a fixed-point problem for $\mathbf{Q}$. We observe that equation (40) has no sink term and therefore has a definite, perturbation-free solution given by $\mathbf{Q} = 0$. This is a generic observation: closing the hierarchy at order $\mathcal{O}(\varepsilon_p^n)$ results in the fixed-point problem for the $(n-1)$th order mode to only have the trivial solution.

2.4.3. Effective diffusion equation.   In the following, we investigate the resulting time-evolution equations for the density for different orders of truncation in the polarisation equation. We start with the first non-trivial case by allowing for terms of order $\mathcal{O}(\varepsilon_p^1)$ for the polarisation, consistent with the choice of globally truncating the hierarchy at order. Here, the adiabatic polarisation reads

$$\sigma_\alpha = -\varepsilon_p\, \Gamma_{\alpha\beta}^{-1} \left[(1 - 4\phi\, \varrho) \nabla_\beta \varrho \right]. \quad (41)$$

Note that since the diffusive parameter ε_D originates from a Laplace operator it only appears at even powers. Thus, there is no term at order $\mathcal{O}(\varepsilon_p \varepsilon_D)$ that could be included at this closure of the polarisation. The mean particle density from equation (30) at this order becomes

$$\begin{aligned}
\frac{\partial}{\partial t} \varrho(\mathbf{x},t) &= \varepsilon_D^2\, \nabla_\alpha \left[(1 + 4\phi\, \varrho(\mathbf{x},t))\, \nabla_\alpha \varrho(\mathbf{x},t) \right] \\
&\quad + \frac{\varepsilon_p^2}{2} \frac{1}{1+\kappa^2}\, \nabla_\alpha \left[(1 - 4\phi\, \varrho(\mathbf{x},t))\, \nabla_\alpha \varrho(\mathbf{x},t) \right]. \quad (42)
\end{aligned}$$

As apparent, the chosen closure scheme results in a time-evolution equation of the mean particle density at order $\mathcal{O}(\varepsilon_p^2)$ and $\mathcal{O}(\varepsilon_D^2)$. Now, by comparing the terms under consideration with the truncated terms we can learn about the regime of validity of equation (42). This gives us that (i) $\varepsilon_p^2 \gg \varepsilon_p^3$, which is consistent with our perturbative assumption of $\varepsilon_p \ll 1$, but we also find that (ii) $\varepsilon_D^2 \gg \varepsilon_p^3$, which tells us that equation (42) is valid in the regime of Pe $\ll 1/\varepsilon_p^{1/2}$. Together (i) and (ii) do not form a precise upper bound to the Péclet number, in fact it can be arbitrarily large and therefore an analysis of the microscopic parameters is essential when using this field-theoretical description.

Equation (42) is written in dimensionless form. Thus we can reintroduce the units of space and time, i.e. τ for time and l_{dist} for space, compare also relation (39). The time-evolution equation for the mean density becomes

$$\frac{\partial}{\partial t} \varrho(\mathbf{x},t) = \nabla \cdot \left[\left(D_{\text{T}}^{\text{eff}}(\varrho) + D_A^{\text{eff}}(\varrho) \right) \nabla \varrho(\mathbf{x},t) \right]. \quad (43)$$

The time evolution of ϱ at this order thus follows an effective diffusion equation [65, 74, 103], where $D_{\text{T}}^{\text{eff}} + D_A^{\text{eff}}$ form the interaction-corrected diffusion coefficients due to thermal and active motion, respectively, and are given by

$$D_{\text{T}}^{\text{eff}}(\varrho) = D_{\text{T}} \left(1 + 4\phi\, \varrho(\mathbf{x},t) \right), \quad (44a)$$

$$D_A^{\text{eff}}(\varrho) = D_A^\omega \left(1 - 4\phi \, \varrho(\mathbf{x},t)\right). \tag{44b}$$

Here D_{T} stands for the thermal (equilibrium) diffusion coefficient, as introduced in the microscopic Langevin description (1*a*). $D_A^\omega = D_A^0/(1 + \kappa^2) = v^2/(2D_{\text{R}}(1 + \kappa^2))$ is the chirality-affected active diffusion coefficient, which describes the ballistic motion. D_A^0 thereby is a characteristic of a purely active particle and relates it to the randomisation of the self-propulsion vector due to rotational diffusion. In accordance with observations in the literature [103–106], active chirality ω rescales this active diffusion D_A^0, as D_A^ω can also be written as $D_A^\omega = v^2 D_{\text{R}}/(2(\omega^2 + D_{\text{R}}^2))$. Remember that $\kappa = \omega/D_{\text{R}}$.

Relations (44*a*) and (44*b*) state that hard-core interactions on the one hand enhance the thermal diffusion and on the other hand reduce the active diffusion. For the passive motion, this is in accordance with the observation that the collective diffusion, in what sense $D_{\text{T}}^{\text{eff}}(\varrho)$ also can be interpreted, gets enhanced by steric interactions [73, 77, 107]. For the active motion similarly the interaction-reduction of the associated diffusion coefficient D_A^{eff} is no surprise. It rather can be regarded as an analytic necessity for the strong theory-, simulation-, and experiment-supported existence of motility-induced phase separations [19, 20, 108–110], i.e. the phenomenon that purely repulsive active systems can phase-separate as a function of particle density. This phenomenon is only possible if the associated diffusion process becomes unstable, i.e. the effective diffusion coefficient can formally turn negative.

2.5. Active Model B +

In this section, we go one step beyond the simplest non-trivial closure approximation by considering mixed terms of the perturbation parameters. This amounts to a much richer field-theoretical description but for the price of a much narrower regime of validity. We find that the dynamics of the mean particle PDF follow the recently introduced AMB+, to which we, therefore have first-principles access for the parameters. Surprisingly here we find that the characteristic AMB+ parameters all change sign as a function of chirality.

2.5.1. Effect of mixed perturbation parameters.

In this work, we treat both the activity as well as the thermal diffusion-induced length scales as small compared to the inter-particle distance. This is justified by the assumption of a dilute system. We are thus formally dealing with a two-parameter perturbation theory. It is therefore natural that besides arguing for the smallness of each of the parameters $\varepsilon_D \ll 1$ and $\varepsilon_p \ll 1$, we also have to specify their relative size. This is only possible by making a third assumption about the Péclet number, the natural scale relating the active and passive motion of a tracer.

We already observed from equation (41) that the diffusion length-scale parameter ε_D only appears in even powers (due to its origin in the second order Laplace operator). Therefore, we can go a step further in the truncation scheme, by considering the polarisation up to order $\mathcal{O}(\varepsilon_p^1 \varepsilon_D^2)$. The adiabatic polarisation can self-consistently be obtained from equation (31) at the desired order to be

$$\sigma_\alpha = -\varepsilon_p \Gamma_{\alpha\beta}^{-1} \left[(1 - 4\phi \, \varrho) \, \nabla_\beta \varrho\right]$$
$$- \varepsilon_p \varepsilon_D^2 \left(\Gamma^{-1}\right)_{\alpha\beta}^2 \left[\nabla_\gamma^2 - 2\phi \left(3\varrho \, \nabla_\gamma^2 - \left(\nabla_\gamma^2 \varrho\right) + 2\left(\nabla_\gamma \varrho\right) \, \nabla_\gamma\right)\right] \nabla_\beta \varrho. \tag{45}$$

We observe here that the higher-order gradient terms of the mean particle density arise together with a matrix product of the chiral matrix $\boldsymbol{\Gamma}$. For an arbitrary vector $\mathbf{a}$, the contraction of the relevant matrices contributes

$$a_\alpha \, \Gamma^{-1}_{\alpha\beta} \, a_\beta = \frac{1}{1+\kappa^2} \, a_\alpha a_\alpha, \tag{46a}$$

$$a_\alpha \, \left(\Gamma^{-1}\right)^2_{\alpha\beta} \, a_\beta = \frac{1-\kappa^2}{\left(1+\kappa^2\right)^2} \, a_\alpha a_\alpha, \tag{46b}$$

where due to the antisymmetric structure of $\boldsymbol{\Gamma}^{-1} = (1-\kappa\varepsilon)/(1+\kappa^2)$ only the respective diagonal elements are relevant in the full contraction.

Inserting this expression for the polarisation into equation (30) for the time-evolution of the mean particle density ϱ, we obtain

$$\frac{\partial}{\partial t}\varrho\left(\mathbf{x},t\right) = \varepsilon_D^2 \nabla_\alpha\left[\left(1+4\phi\,\varrho\right)\nabla_\alpha\varrho\right] + \frac{\varepsilon_p^2}{2}\frac{1}{1+\kappa^2}\nabla_\alpha\left[\left(1-4\phi\,\varrho\right)\nabla_\alpha\varrho\right]$$
$$+ \frac{\varepsilon_p^2\varepsilon_D^2}{2}\frac{1-\kappa^2}{\left(1+\kappa^2\right)^2}\nabla_\alpha\left[\nabla_\gamma^2 - 2\phi\left(3\varrho\nabla_\gamma^2 - \left(\nabla_\gamma^2\varrho\right) + 2\left(\nabla_\gamma\varrho\right)\nabla_\gamma\right)\right]\nabla_\alpha\varrho. \tag{47}$$

It is now obvious that, to obtain this field-theoretical description for the density compared to equation (42), we further encounter the mixed term of order $\mathcal{O}(\varepsilon_p^2\varepsilon_D^2)$, which is only possible if this term is assumed to be much greater then the disregarded terms, e.g. that of order $\mathcal{O}(\varepsilon_p^3)$. An easy algebraic analysis shows that this is only possible when $\mathrm{Pe} \ll \varepsilon_D \ll 1$ due to the perturbative closure scheme.

2.5.2. Active Model B +. If we reintroduce physical units for space and time, i.e. τ for the time l_{dist} for the space, compare also relation (39), we can arrange equation (47) in the form

$$\frac{\partial}{\partial t}\varrho\left(\mathbf{x},t\right) = a\nabla^2\varrho + b\nabla^2\left(\varrho^2\right) - k_0\nabla^4\varrho - k_1\left[\nabla^2\left(\nabla\varrho\right)^2 + 2\nabla^2\left(\varrho\nabla^2\varrho\right)\right]$$
$$+ \lambda\nabla^2\left(\nabla\varrho\right)^2 - \xi\nabla\cdot\left(\nabla\varrho\right)\left(\nabla^2\varrho\right), \tag{48}$$

where

$$a = D_{\mathrm{T}} + D_A^\omega, \tag{49a}$$

$$b = 2\phi\left(D_{\mathrm{T}} - D_A^\omega\right), \tag{49b}$$

$$\lambda = \phi D_A^\omega D_{\mathrm{T}}\frac{1-\kappa^2}{1+\kappa^2}, \tag{49c}$$

$$\xi = -8\phi D_A^\omega D_{\mathrm{T}}\frac{1-\kappa^2}{1+\kappa^2}, \tag{49d}$$

$$k\left[\varrho\right] = D_A^\omega D_{\mathrm{T}}\frac{1-\kappa^2}{1+\kappa^2}\left(-1+6\phi\,\varrho\left(\mathbf{x},t\right)\right), \tag{49e}$$

and $k[\varrho] = k_0 + 2k_1\,\varrho(\mathbf{x},t)$. Equation (48) is known as the (deterministic) AMB+ [53–55, 111], and can be rearranged into the form

$$\frac{\partial}{\partial t}\varrho\left(\mathbf{x},t\right) = -\nabla\cdot\left[-\nabla\left(\frac{\delta\mathcal{F}}{\delta\varrho} + \lambda\left(\nabla\varrho\right)^2\right) + \xi\left(\nabla\varrho\right)\left(\nabla^2\varrho\right)\right], \tag{50a}$$

where

$$\mathcal{F}\left[\varrho\right] = \int \mathrm{d}\mathbf{r}\left(f_0\left[\varrho\right] + \frac{k\left[\varrho\right]}{2}\left(\nabla\varrho\right)^2\right) \tag{50b}$$

is the free-energy functional and $f_0[\varrho] = a/2\,\varrho^2 + b/3\,\varrho^3$ is the bulk free-energy density. Note that typically $\varrho' = \varrho - \varrho_{\mathrm{MF}}$ is taken to be the order parameter, where ϱ_{MF} is the mean-field critical value of the density. If one does so, a term $\propto \varrho^3$ is forbidden by symmetry in f_0, but we instead work with the density ϱ itself. Equation (50) was first written down based on phenomenologically accounting for systems with broken detailed-balance to lowest order terms in [53, 55].

2.5.3. First-principles expressions for field-theoretical parameters. The parameter $k[\varrho]$ in the free energy is known as the Cahn-Hilliard parameter [112]. When first introduced, this parameter was the minimal attempt in an equilibrium model to extend the bulk free energy $\mathcal{F}$ to further include density-gradient-induced inhomogeneities into the description. Via this very successful approach, field theories could nicely capture phase-separation dynamics in equilibrium models [52, 113]. In the general formulation, $k[\varrho]$ is density-dependent, and a Taylor expansion to lowest order in the density gives $k[\varrho] = k_0 + 2k_1\varrho$. The coefficients k_0 and k_1 are found in our model by comparing the first-principles time-evolution equation (47) with the phenomenological equation of the AMB+ (48). From an equilibrium perspective, it might appear surprising that from equation (49*e*) we find that $k_0 < 0$ for a non-chiral system ($\kappa = 0$) and thus also $k[\varrho] < 0$ to lowest order. In an equilibrium field theory, this would lead to an unbounded free energy and the non-physical possibility of a system minimising its free energy by creating more and more interfaces due to phase separation. But for an active field theory such as the AMB+, the time evolution is not solely governed by a free-energy structure. Further terms $\propto \lambda, \xi$ balance the free-energy governed evolution, and thus equilibrium intuition can fail. Note also that in our first-principles derivation for active systems $k[\varrho] \propto D_A^\omega$, and therefore this quantity vanishes as the model is approaching an equilibrium situation ($D_A^\omega \to 0$). Finally, the observation of $k_0 < 0$ is consistent with other works on the AMB+ [53, 57], but (active) chirality adds a new perspective, since here k_0 and k_1 change sign as $\kappa > 1$.

The observation, that the coefficients which are induced by activity and interactions ($\lambda, \xi, k[\varrho] \propto \phi D_A^\omega$) can change their sign as a function of chirality is rather surprising. From the Langevin dynamics and the integration procedures, we would have not expected that chirality and interactions could interplay such, that they lead to physical consequences. In the hard-core interacting scenario the angular coordinate is not altered by the excluded-volume interaction of the spatial coordinate, and therefore chirality does not affect the time-evolution of the full one-body PDF beyond the (trivial) interaction-free terms, as can be seen from equation (25). Any interplay of spatial and angular coordinates is only introduced in the projection on the hydrodynamic modes. We can nevertheless qualitatively justify why the change in the behaviour happens at $\kappa = 1$. Similar to the rotational diffusion coefficient, which introduces a time scale in the system $\tau = \tau_{\mathrm{diff}} = 1/D_{\mathrm{R}}$, the active chirality introduces a time scale as well, namely, $\tau_{\mathrm{act}} = 1/\omega$. These time scales represent the noise and the deterministic circular contribution to the active motion of the particle, respectively. Hence the parameter $\kappa = \omega/D_{\mathrm{R}} = \tau_{\mathrm{diff}}/\tau_{\mathrm{act}}$ measures which contribution is dominating the motion of a particle, similar to what was recently reported in [105, 114]. That means that $\kappa < 1$ corresponds to a system, in which the diffusive motion dominates the active particle, whereas $\kappa > 1$ corresponds to a deterministic-circular-motion determined motion, see also figure 3. Interestingly, when both effects are of equal magnitude, $\lambda, \xi, k[\varrho] = 0$, the system again behaves as described by the effective diffusion dynamics of equation (43).

The phenomenological parameters λ and ξ represent the active generalisations of equilibrium Model B [51] ($\partial\varrho/\partial t = -\nabla \mathbf{J}_{\mathrm{eq}} = \nabla(\delta\mathcal{F}[\varrho]/\delta\varrho)$, where ϱ is the conserved order parameter, $\mathbf{J}_{\mathrm{eq}}$ the equilibrium (deterministic) current and $\mathcal{F}$ is the equilibrium free energy). Since
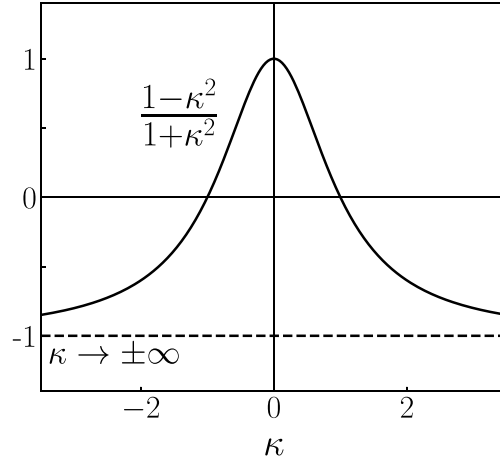
Figure 3. For ACPs one can define the parameter $\kappa = \omega/D_{\mathrm{R}}$, which is a measure of active chirality ω versus rotational diffusion D_{R} of the particle. In a related context, this parameter is known as the *oddness* parameter [77, 89, 92, 94]. The characteristic parameters of the AMB+, λ, $-\xi$ and $k[\varrho]$ all scale $\propto (1-\kappa^2)/(1+\kappa^2)$, see also equations (49*c*)–(49*e*). Thus, they are positive as long as $|\omega| < D_{\mathrm{R}}$, i.e. the circular motion is dominated by diffusion, and are negative for $|\omega| > D_{\mathrm{R}}$, i.e. the motion is dominated by activity. Note that the sign of ω accounts for the clockwise or counterclockwise direction of the active chirality.

this model was constructed on the basic principle of the system to obey detailed-balance, to describe active matter, this restriction had to be overcome. A first step in the development of active field theories was the so-called *Active Model B (AMB)* [85, 115], where $\lambda \neq 0$ but $\xi = 0$. This model still attracts interest as it represents the first step towards an active field theory [116, 117], but it was shown that even though quantitatively the coexisting liquid and vapour densities are changed, the AMB cannot report any qualitative changes in the coarsening dynamics as compared to the known dynamics found by phenomenologically introducing activity in the Model B [115].

The sought qualitative changes in the phase-separation dynamics of active matter could thereafter be found by the generalised AMB+ where $\lambda \neq 0$ and additionally $\xi \neq 0$. Similarly to the AMB, the AMB+ as the most general isotropic model at this order goes beyond the typical free-energy structure of Model B by $\lambda \neq 0$. For the AMB, the λ-term defines a (local) non-equilibrium chemical potential $\mu_{\mathrm{neq}} = \delta\mathcal{F}/\delta\varrho + \lambda(\nabla\varrho)^2$, since the current is still of a gradient form. For the AMB+ instead the ξ-induced current cannot be put into a gradient structure anymore and therefore allows for circulating real-space currents $\nabla \wedge \mathbf{J}_{\mathrm{neq}} \propto \xi$. Further, as a result of the non-gradient structure of the current, the non-equilibrium chemical potential becomes non-local [53, 54] and therefore amounts to fundamental differences of AMB and AMB+. As these studies suggest, this non-locality seems to be a necessary ingredient to describe the behaviour of active matter from a field theoretical perspective.

Finally, it is interesting to note that as a result of our first principles approach, the AMB+ appears as the most natural choice of an active field theory which relies on an expansion in terms of density gradients. We observe from equations (49*c*) and (49*d*) that $\lambda = -8\xi$. Thus, it is not reasonable to include one but leave out the other parameter in the field-theoretical description, similarly to what was pointed out recently [59]. We further observe

that, as argued phenomenologically, both $\lambda, \xi \propto D_T D_A^\omega$, such that the AMB+ reduces to an interaction-corrected, passive diffusion equation for $D_A^\omega \to 0$. Interestingly, it also reduces to the non-equilibrium effective diffusion equation (43) as $D_T \to 0$, i.e. when the thermal motion becomes negligible compared to the activity. Lastly, as expected, λ and ξ are only present in an interacting system ($\lambda, \xi \propto \phi$), since they are known to alter the phase-separation dynamics.

3. Conclusion

We here extended a geometric approach [62–64, 73, 77] to deal with particle-particle interactions by restricting the domain of definition of their diffusing centrers. Forbidden overlaps of the particles correspond to forbidden areas in the domain, creating a configuration space with inner moving boundaries. Based on that we derived an effective time-evolution equation for the full one-body PDF. We proceeded by projecting the full one-body PDF onto its angular modes, which resulted in a coupled hierarchy of hydrodynamic modes. By scrutinising the underlying assumptions we turned the closure scheme into a perturbation problem and found effective time-evolution equations (field-theories) for the mean particle density.

One major result of our work is the following. We observed that this procedure provides us with first-principles access to the otherwise phenomenological parameters of field-theoretical descriptions of active matter. We find that, beyond an effective diffusive description, the microscopically best justified theory of a continuous model is the AMB+ [53, 55]. This was also reported in another recent first-principles derivation of the AMB+ for non-chiral ABPs [57]. From a technical point of view, our work unravels the theoretical necessities of the regimes of validity to obtain such a coarse-grained model for the description of active matter. Specifically, we find that when neglecting the time evolution of higher modes such as polarisation or nematic order, in the so-called adiabatic limit, the AMB+ model is microscopically justified only in the limit of low Péclet numbers, i.e. when thermal diffusion dominates active motion. Whether the microscopic justification for the AMB+ model can be extended to regimes of higher activity is a subject of future research.

The main prediction of this work is that active chirality has a non-trivial influence on the dynamics of the mean particle PDF $\varrho(\mathbf{x}, t)$. Even though in the simplest version of the ACP model chirality is not altered by particle interactions (see again the Langevin description in equation (1)) and hence its effect on the full one-body level is rather superficial, it becomes most prominent when integrating out the angular dependence of the full one-body PDF $p(\mathbf{x}, \theta, t)$. We find that an odd tensor [73, 94] $\mathbf{\Gamma} = (1 + \kappa \varepsilon)$ emerges, where chirality defines the off-diagonal elements $\kappa = \omega/D_R$. Powers of that tensor, and hence chirality, eventually, can change the sign of all activity-induced coefficients of the AMB+, λ, and ξ, as well as the Cahn-Hilliard coefficient $k[\varrho]$. Restricted to the effective diffusion dynamics similar to equation (43) the alternative approach of [103] did not report this phenomenon, as their method to incorporate interactions assumes translational and rotational invariance and therefore can only treat chirality pertubatively. Whether the sign-change of the coefficients has implications for the phase-transition dynamics, however, cannot be addressed within our model due to its restricted validity to regimes away from phase transitions for particles with repulsive interactions. In the regime of validity of our AMB+ model, numerical solutions of equation (50) with the parameters of equation (49) only admit a homogeneous phase, see figure 4.

The systematic analysis presented in this work allows us to further include the effect of nematic order on the time-evolution of the mean particle PDF, but it would amount to a field-theoretical description at an even higher order than the AMB+ (which is already at fourth order in density gradients). The AMB+ was recently shown to be deducible from such a (stable)
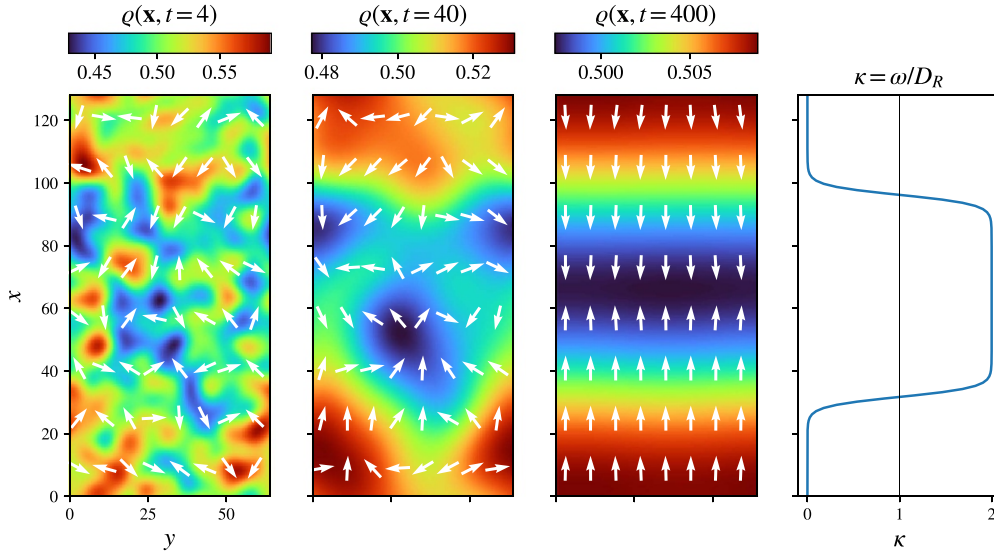
Figure 4. We numerically solve the AMB+ dynamics of equation (50) with the coefficients given by equation (49) for different times on a periodic two-dimensional lattice [118]. We chose the system parameters for the passive and active diffusivity as $D_T/D_0 = 1$, $D_A^0/D_0 = 0.05$ rescaled by some reference diffusivity D_0, and the volume fraction as $\phi = 0.1$. With this choice of parameters we stay within the regime of validity of our derived AMB+ dynamics, i.e. Pe $= \sqrt{2D_A^0/D_T} \ll 1$ and $\phi \ll 1$. Starting from a random initial distribution, the density quickly relaxes to a homogeneous steady state $\varrho(\mathbf{x}, t) = \varrho_0 = 0.5$, where the white arrows indicate the direction of the normalised diffusive flux (note the different magnitudes of the density variation at different times). Different regions of active chirality $\kappa = \omega/D_R$ only affect the density relaxation at later times ($t = 40, 400$), as only higher-order density gradient terms of the AMB+ are affected by the sign-change of the coefficients. In the plots, time is rescaled by the natural time scale $\tau = 1/D_R$ and space is measured in units of $\sqrt{D_0\tau}$.

higher-order model [119], where it was shown that the AMB+ itself is unstable for sufficiently high order parameters. We suspect a similar behaviour if one performed the corresponding closure scheme on the level of the nematic order in our theory, which we leave for future work.

Inspired by a rich behaviour of complex macroscopic phenomena in active matter, an additional step would be to directly couple the chirality to the spatial interaction of the particles [120, 121]. Motivated from an orientation-dependent potential of the form $\hat{\mathbf{e}}(\theta_i) \cdot \hat{\mathbf{e}}(\theta_j)$ for the propulsion vectors of particles i and j [122], we could consider additional aligning interactions together with active chirality from an analytic perspective on the restricted domain resembling steric interactions. A recent work considered the numerical effects of such alignment for phenomena like motility-induced phase separation and the flocking of ACPs [95].

Data availability statement

In the manuscript, we outline the procedure to generate the numerical data presented in figure 4. These data are available upon reasonable request, as their creation is fully reproducible with the details in the manuscript.

Acknowledgments

Appendix. Evaluation of integral (7)

In the main text, in equation (7) we are left with evaluating a boundary integral, in which integration and differentiation are with respect to different particle labels. Hence a use of the Gaussian divergence theorem is not possible straightforwardly. Instead, we use an extended version of the Reynolds transport theorem, which usually allows for the time-differentiation of an integral quantity, where the integration volume V itself is time-dependent $V = V(t)$. For an arbitrary space- and time-dependent function $f = f(\mathbf{x}, t)$, the theorem in this context reads

$$\frac{\partial}{\partial t} \int_{V(t)} \mathrm{d}\mathbf{x} \, f = \int_{V(t)} \mathrm{d}\mathbf{x} \, \frac{\partial f}{\partial t} + \int_{\partial V(t)} \mathrm{d}S_{\mathbf{x}} \, \left(\mathbf{n} \cdot \mathbf{v}_{\partial V(t)} \right) f, \tag{A.1}$$

where $\mathbf{v}_{\partial V(t)} = \mathbf{v}_{\partial V(t)}(\mathbf{x}, t)$ is the velocity of an element of the moving boundary $\partial V(t)$ and $\mathrm{d}S_{\mathbf{x}} \, \mathbf{n}$ is the outward area element of the boundary at time t.

This theorem can be extended to cases, in which the integration volume V is space-dependent ($V = V(\mathbf{x})$, but of a constant shape) and we are interested in taking the divergence of the integral with respect to that coordinate $\mathbf{x}$. For a vector-valued function $\mathbf{f} = \mathbf{f}(\mathbf{x}, \mathbf{y}, t)$, the extended transport theorem reads

$$\nabla_{\mathbf{x}} \cdot \int_{V(\mathbf{x})} \mathrm{d}\mathbf{y} \, \mathbf{f} = \int_{V(\mathbf{x})} \mathrm{d}\mathbf{y} \, \nabla_{\mathbf{x}} \cdot \mathbf{f} + \int_{\partial V(\mathbf{x})} \mathrm{d}S_{\mathbf{y}} \, \mathbf{n}_{\mathbf{y}} \cdot \mathbf{f}. \tag{A.2}$$

The proof of this relation can be found in [77]. We will apply this theorem to the reduced configuration space $\Lambda(\chi_1) = \Omega \setminus B_{\varepsilon_d}(\mathbf{x}_1) \times [0, 2\pi)$, where the space-dependence is on $B_{\varepsilon_d}(\mathbf{x}_1)$, the disk of radius ε_d centred at $\mathbf{x}_1$. Therefore, only $\partial B_{\varepsilon_d}(\mathbf{x}_1)$ contributes a moving boundary, and hence a boundary integral in equation (A.2). We now apply the extended Reynolds transport theorem to evaluate equation (7). Note here that $P_2(t) = P_2(\chi_1, \chi_2, t)$ for a shortness of notation. We find the result

$$\int_{\Lambda(\chi_1)} \mathrm{d}\chi_2 \, \nabla_{\chi_1} \cdot \left[\mathbf{D} \nabla_{\chi_1} - \mathbf{f}(\theta_1) \right] P_2(t) = \nabla_{\chi_1} \cdot \int_{\Lambda(\chi_1)} \mathrm{d}\chi_2 \, \left[\mathbf{D} \nabla_{\chi_1} - \mathbf{f}(\theta_1) \right] P_2(t)$$

$$- \int_0^{2\pi} \mathrm{d}\theta_2 \int_{\partial B_{\varepsilon_d}(\mathbf{x}_1)} \mathrm{d}S_2 \, \mathbf{n}_2 \cdot \left[D_{\mathrm{T}} \nabla_1 - v\hat{\mathbf{e}}(\theta_1) \right] P_2(t). \tag{A.3}$$

The moving boundary only arises in the spatial part of $\chi_1 = (\mathbf{x}_1, \theta_1)$, and thus we are only left with the spatial part of the diffusion matrix $\mathbf{D} = \mathrm{diag}(D_{\mathrm{T}}, D_{\mathrm{T}}, D_{\mathrm{R}})$ and drift term $\mathbf{f}(\theta_1) = (v\hat{\mathbf{e}}(\theta_1), \omega)^{\mathrm{T}}$. We again apply the extended theorem for the first term in the evaluated integral

$$\nabla_{\chi_1} \cdot \int_{\Lambda(\chi_1)} \mathrm{d}\chi_2 \, \left[\mathbf{D} \nabla_{\chi_1} P_2(t) \right] = \nabla_{\chi_1} \cdot \mathbf{D} \nabla_{\chi_1} \int_{\Lambda(\chi_1)} \mathrm{d}\chi_2 \, P_2(t)$$

$$- \nabla_1 \cdot \int_0^{2\pi} \mathrm{d}\theta_2 \int_{\partial B_{\varepsilon_d}(\mathbf{x}_1)} \mathrm{d}S_2 \, \mathbf{n}_2 \, \left[D_{\mathrm{T}} \, P_2(t) \right]. \tag{A.4}$$

We are left with evaluating the originating boundary integral combined with the boundary integral of equation (A.3). Therefore we jointly use the divergence theorem and the transport theorem, paying respect to the specific integration volumes in the following steps. First we apply the divergence theorem on the volume $\Omega \setminus B_{\varepsilon_d}(\mathbf{x}_1)$ 'backwards',

$$
\begin{aligned}
-\nabla_1 \cdot \int_0^{2\pi} \mathrm{d}\theta_2 \int_{\partial B_{\varepsilon_d}(\mathbf{x}_1)} \mathrm{d}S_2 \, \mathbf{n}_2 \left[D_\mathrm{T} P_2(t)\right] &= -D_\mathrm{T} \nabla_1 \cdot \int_{\Lambda(\chi_1)} \mathrm{d}\chi_2 \, \nabla_2 P_2(t) \\
&+ D_\mathrm{T} \nabla_1 \cdot \int_0^{2\pi} \mathrm{d}\theta_2 \int_{\partial\Omega} \mathrm{d}S_2 \, \mathbf{n}_2 P_2(t).
\end{aligned} \tag{A.5}
$$

Using the generalised transport theorem, the first integral on the right-hand side of equation (A.5) can be rewritten as

$$
\begin{aligned}
-D_\mathrm{T} T \nabla_1 \cdot \int_{\Lambda(\chi_1)} \mathrm{d}\chi_2 \, \nabla_2 P_2(t) &= -D_\mathrm{T} \int_{\Lambda(\chi_1)} \mathrm{d}\chi_2 \, \nabla_1 \cdot \nabla_2 P_2(t) \\
&- D_\mathrm{T} \int_0^{2\pi} \mathrm{d}\theta_2 \int_{\partial B_{\varepsilon_d}(\mathbf{x}_1)} \mathrm{d}S_2 \, \mathbf{n}_2 \cdot \nabla_2 P_2(t).
\end{aligned} \tag{A.6}
$$

Note again here that only $B_{\varepsilon_d}(\mathbf{x}_1)$ is space-dependent and thus contributes a boundary term in the generalised transport theorem. Since integration and differentiation are with respect to the same particle label in the first integral on the right-hand side of equation (A.6), we can apply the divergence theorem 'forwards'

$$
\begin{aligned}
-D_\mathrm{T} \int_{\Lambda(\chi_1)} \mathrm{d}\chi_2 \, \nabla_1 \cdot \nabla_2 P_2(t) &= -D_\mathrm{T} \int_0^{2\pi} \mathrm{d}\theta_2 \int_{\partial\Omega} \mathrm{d}S_2 \, \mathbf{n}_2 \cdot \nabla_1 P_2(t) \\
&- D_\mathrm{T} \int_0^{2\pi} \mathrm{d}\theta_2 \int_{\partial B_{\varepsilon_d}(\mathbf{x}_1)} \mathrm{d}S_2 \, \mathbf{n}_2 \cdot \nabla_1 P_2(t).
\end{aligned} \tag{A.7}
$$

Note here that when applying the divergence theorem the box-boundary $\partial\Omega$ contributes a surface integral. As the box-boundary does not explicitly depend on $\mathbf{x}_1$, the partial differential operator ∇_1 can be moved outside the integral (without creating another boundary term) and we observe that it cancels with the second integral on the right-hand side of equation (A.5). We are thus left with the two integrals on the inner boundary $\partial B_{\varepsilon_d}(\mathbf{x}_1)$ and find that

$$
\begin{aligned}
&- \nabla_1 \cdot \int_0^{2\pi} \mathrm{d}\theta_2 \int_{\partial B_{\varepsilon_d}(\mathbf{x}_1)} \mathrm{d}S_2 \, \mathbf{n}_2 \left[D_\mathrm{T} P_2(t)\right] \\
&= -D_\mathrm{T} \int_0^{2\pi} \mathrm{d}\theta_2 \int_{\partial B_{\varepsilon_d}(\mathbf{x}_1)} \mathrm{d}S_2 \, \mathbf{n}_2 \cdot (\nabla_1 + \nabla_2) P_2(t).
\end{aligned} \tag{A.8}
$$

The rewriting of the boundary term of equation (A.4) finally enables us to combine the result with the term in equation (A.3). Using the definition of the full one-body PDF $p(\chi_1, t) = \int_{\Lambda(\chi_1)} \mathrm{d}\chi_2 \, P_2(\chi_1, \chi_2, t)$, equation (A.3) thus becomes

$$
\begin{aligned}
\int_{\Lambda(\chi_1)} \mathrm{d}\chi_2 \, \nabla_{\chi_1} \cdot [\mathbf{D}\nabla_{\chi_1} - \mathbf{f}(\theta_1)] P_2(t) &= \nabla_{\chi_1} \cdot [\mathbf{D}\nabla_{\chi_1} - \mathbf{f}(\theta_1)] p(\chi_1, t) \\
&- \int_{\partial B_{\varepsilon_d}(\mathbf{x}_1)} \mathrm{d}S_2 \, \mathbf{n}_2 \left[D_\mathrm{T}(2\nabla_1 - \nabla_2) + v\hat{\mathbf{e}}(\theta_1)\right] P_2(t),
\end{aligned} \tag{A.9}
$$

which constitutes the result of equation (7) in the main text.

ORCID iDs

Erik Kalz ⓘ https://orcid.org/0000-0003-3294-7365
Abhinav Sharma ⓘ https://orcid.org/0000-0002-6436-3826
Ralf Metzler ⓘ https://orcid.org/0000-0002-6013-7020

References

[1] van Teeffelen S and Löwen H 2008 *Phys. Rev.* E **78** 020101
[2] Mijalkov M and Volpe G 2013 *Soft Matter* **9** 6376–81
[3] Volpe G, Gigan S and Volpe G 2014 *Am. J. Phys.* **82** 659–64
[4] Löwen H 2016 *Eur. Phys. J. Spec. Top.* **225** 2319–31
[5] Sevilla F J 2016 *Phys. Rev.* E **94** 062120
[6] Schimansky-Geier L, Mieth M, Rosé H and Malchow H 1995 *Phys. Lett.* A **207** 140–6
[7] Schweitzer F, Ebeling W and Tilch B 1998 *Phys. Rev. Lett.* **80** 5044–7
[8] Ebeling W, Schweitzer F and Tilch B 1999 *BioSystems* **49** 17–29
[9] Romanczuk P, Bär M, Ebeling W O, Lindner B and Schimansky-Geier L 2012 *Eur. Phys. J. Spec. Top.* **202** 1–162
[10] Ramaswamy S 2010 *Annu. Rev. Condens. Matter Phys.* **1** 323–45
[11] Marchetti M C, Joanny J F, Ramaswamy S, Liverpool T B, Prost J, Rao M and Simha R A 2013 *Rev. Mod. Phys.* **85** 1143–89
[12] Jülicher F, Grill S W and Salbreux G 2018 *Rep. Prog. Phys.* **81** 076601
[13] Ebbens S J and Howse J R 2010 *Soft Matter* **6** 726–38
[14] Buttinoni I, Volpe G, Kümmel F, Volpe G and Bechinger C 2012 *J. Phys.: Condens. Matter* **24** 284129
[15] Feldmann D, Arya P, Lomadze N, Kopyshev A and Santer S 2019 *Appl. Phys. Lett.* **115** 263701
[16] Elgeti J, Winkler R G and Gompper G 2015 *Rep. Prog. Phys.* **78** 056601
[17] Shaebani M R, Wysocki A, Winkler R G, Gompper G and Rieger H 2020 *Nat. Rev. Phys.* **2** 181–99
[18] Tailleur J and Cates M E 2008 *Phys. Rev. Lett.* **100** 218103
[19] Fily Y and Marchetti M C 2012 *Phys. Rev. Lett.* **108** 235702
[20] Buttinoni I, Bialké J, Kümmel F, Löwen H, Bechinger C and Speck T 2013 *Phys. Rev. Lett.* **110** 238301
[21] Palacci J, Sacanna S, Steinberg A P, Pine D J and Chaikin P M 2013 *Science* **339** 936–40
[22] Speck T, Bialké J, Menzel A M and Löwen H 2014 *Phys. Rev. Lett.* **112** 218304
[23] Cates M E and Tailleur J 2015 *Annu. Rev. Condens. Matter Phys.* **6** 219–44
[24] Schnitzer M J, Block S M, Berg H C and Purcell E M 1990 *Symp. Society for General Microbiology* vol 46 pp 15–33
[25] Vuijk H D, Merlitz H, Lang M, Sharma A and Sommer J U 2021 *Phys. Rev. Lett.* **126** 208102
[26] Levis D and Liebchen B 2019 *Phys. Rev.* E **100** 012406
[27] Levis D, Diaz-Guilera A, Pagonabarraga I and Starnini M 2020 *Phys. Rev. Res.* **2** 032056
[28] Vicsek T, Czirók A, Ben-Jacob E, Cohen I and Shochet O 1995 *Phys. Rev. Lett.* **75** 1226–9
[29] Czirók A and Vicsek T 2000 *Physica* A **281** 17–29
[30] Chaté H, Ginelli F, Grégoire G, Peruani F and Raynaud F 2008 *Eur. Phys. J.* B **64** 451–6
[31] Banerjee D, Souslov A, Abanov A G and Vitelli V 2017 *Nat. Commun.* **8** 1573
[32] Soni V, Bililign E S, Magkiriadou S, Sacanna S, Bartolo D, Shelley M J and Irvine W T M 2019 *Nat. Phys.* **15** 1188–94
[33] Massana-Cid H, Levis D, Hernández R J H, Pagonabarraga I and Tierno P 2021 *Phys. Rev. Res.* **3** L042021
[34] Ma Z and Ni R 2022 *J. Chem. Phys.* **156** 021102
[35] Lei Q L, Ciamarra M P and Ni R 2019 *Sci. Adv.* **5** eaau7423
[36] Kuroda Y and Miyazaki K 2023 *J. Stat. Mech.* 103203
[37] Liebchen B and Levis D 2017 *Phys. Rev. Lett.* **119** 058002
[38] Caporusso C B, Gonnella G and Levis D 2024 *Phys. Rev. Lett.* **132** 168201
[39] Reichhardt C and Reichhardt C J O 2019 *J. Chem. Phys.* **150** 064905
[40] Berg H C and Turner L 1990 *Biophys. J.* **58** 919–30
[41] DiLuzio W R, Turner L, Mayer M, Garstecki P, Weibel D B, Berg H C and Whitesides G M 2005 *Nature* **435** 1271–4

[42] Lauga E, DiLuzio W R, Whitesides G M and Stone H A 2006 *Biophys. J.* **90** 400–12
[43] Riedel I H, Kruse K and Howard J 2005 *Science* **309** 300–3
[44] Friedrich B M and Jülicher F 2007 *Proc. Natl. Acad. Sci.* **104** 13256–61
[45] Kümmel F, ten Hagen B, Wittkowski R, Buttinoni I, Eichhorn R, Volpe G, Löwen H and Bechinger C 2013 *Phys. Rev. Lett.* **110** 198302
[46] Arora P, Sood A K and Ganapathy R 2021 *Sci. Adv.* **7** eabd0331
[47] Scholz C, Engel M and Pöschel T 2018 *Nat. Commun.* **9** 931
[48] Yang X, Ren C, Cheng K and Zhang H P 2020 *Phys. Rev.* E **101** 022603
[49] López-Castaño M A, Márquez Seco A, Márquez Seco A, Rodríguez-Rivas A and Reyes F V 2022 *Phys. Rev. Res.* **4** 033230
[50] Jennings H S 1901 *Am. Nat.* **35** 369–78
[51] Hohenberg P C and Halperin B I 1977 *Rev. Mod. Phys.* **49** 435–79
[52] Bray A J 2002 *Adv. Phys.* **51** 481–587
[53] Tjhung E, Nardini C and Cates M E 2018 *Phys. Rev.* X **8** 031080
[54] Cates M E and Nardini C 2023 *Phys. Rev. Lett.* **130** 098203
[55] Nardini C, Fodor É, Tjhung E, van Wijland F, Tailleur J and Cates M E 2017 *Phys. Rev.* X **7** 021007
[56] Speck T 2022 *Phys. Rev.* E **105** 064601
[57] te Vrugt M, Bickmann J and Wittkowski R 2023 *J. Phys.: Condens. Matter* **35** 313001
[58] Zheng Y, Klatt M A and Löwen H 2023 arXiv:2310.03107
[59] Rapp L, Bergmann F and Zimmermann W 2019 *Eur. Phys. J.* E **42** 57
[60] Fruchart M, Scheibner C and Vitelli V 2023 *Annu. Rev. Condens. Matter Phys.* **14** 471–510
[61] Huang X, Farrell J H, Friedman A J, Zane I, Glorioso P and Lucas A 2023 arXiv:2310.12233v1
[62] Bruna M and Chapman S J 2012 *J. Chem. Phys.* **137** 204116
[63] Bruna M and Chapman S J 2012 *Phys. Rev.* E **85** 011103
[64] Bruna M, Burger M, Esposito A and Schulz S M 2022 *SIAM J. Appl. Math.* **82** 1635–60
[65] Cates M E and Tailleur J 2013 *Europhys. Lett.* **101** 20010
[66] Solon A P, Cates M E and Tailleur J 2015 *Eur. Phys. J. Spec. Top.* **224** 1231–62
[67] Cercignani C, Illner R and Pulvirenti M 1994 *The Mathematical Theory of Dilute Gases* (Springer)
[68] Bertin E, Droz M and Grégoire G 2006 *Phys. Rev.* E **74** 022101
[69] Bertin E, Droz M and Grégoire G 2009 *J. Phys. A: Math. Theor.* **42** 445001
[70] Liebchen B and Levis D 2022 *Europhys. Lett.* **139** 67001
[71] Bruna M and Chapman S J 2014 *Bull. Math. Biol.* **76** 947–82
[72] Bruna M and Chapman S J 2015 *SIAM J. Appl. Math.* **75** 1648–74
[73] Kalz E, Vuijk H D, Abdoli I, Sommer J U, Löwen H and Sharma A 2022 *Phys. Rev. Lett.* **129** 090601
[74] Bialké J, Löwen H and Speck T 2013 *Europhys. Lett.* **103** 30008
[75] Speck T, Menzel A M, Bialké J and Löwen H 2015 *J. Chem. Phys.* **142** 224109
[76] Risken H 1989 *The Fokker-Planck Equation* 2nd edn (Springer)
[77] Kalz E 2022 *Diffusion Under the Effect of Lorentz Force* (Springer Spektrum Wiesbaden)
[78] Bruna M 2012 Excluded-volume effects in stochastic models of diffusion *PhD Thesis* University of Oxford St. Anne's College
[79] Bender C M and Orszag S A 1999 *Advanced Mathematical Methods for Scientists and Engineers I* (Springer)
[80] Bruna M, Chapman S J and Robinson M 2017 *SIAM J. Appl. Math.* **77** 2294–316
[81] Bickmann J and Wittkowski R 2020 *J. Phys.: Condens. Matter* **32** 214001
[82] te Vrugt M, Löwen H and Wittkowski R 2020 *Adv. Phys.* **69** 121–247
[83] Archer A J and Evans R 2004 *J. Chem. Phys.* **121** 4246–54
[84] Burger M and Schulz S 2023 arXiv:2309.17326
[85] Stenhammar J, Tiribocchi A, Allen R J, Marenduzzo D and Cates M E 2013 *Phys. Rev. Lett.* **111** 145702
[86] Sharma A and Brader J M 2016 *J. Chem. Phys.* **145** 161101
[87] te Vrugt M and Wittkowski R 2020 *AIP Adv.* **10** 035106
[88] de Gennes P G and Prost J 1995 *The Physics of Liquid Crystals* 2nd edn (Oxford University Press)
[89] Muzzeddu P L, Vuijk H D, Löwen H, Sommer J U and Sharma A 2022 *J. Chem. Phys.* **157** 134902
[90] Sharma A and Brader J M 2017 *Phys. Rev.* E **96** 032604
[91] Merlitz H, Vuijk H D, Brader J M, Sharma A and Sommer J U 2018 *J. Chem. Phys.* **148** 194116
[92] Hargus C, Epstein J M and Mandadapu K K 2021 *Phys. Rev. Lett.* **127** 178001

[93] Han M, Fruchart M, Scheibner C, Vaikuntanathan S, de Pablo J J and Vitelli V 2021 *Nat. Phys.* **17** 1260–9

[94] Kalz E, Vuijk H D, Sommer J U, Metzler R and Sharma A 2024 *Phys. Rev. Lett.* **132** 057102

[95] Kreienkamp K L and Klapp S H L 2022 *New J. Phys.* **24** 123009

[96] Li Y I, Garcia-Millan R, Cates M E and Fodor É 2023 *Europhys. Lett.* **142** 57004

[97] Muzzeddu P L, Roldán É, Gambassi A and Sharma A 2023 *Europhys. Lett.* **142** 67001

[98] Yllanes D, Leoni M and Marchetti M C 2017 *New J. Phys.* **19** 103026

[99] Ackerson B J and Fleishman L 1982 *J. Chem. Phys.* **76** 2675–9

[100] Liebchen B, Cates M E and Marenduzzo D 2016 *Soft Matter* **12** 7259–64

[101] Tschopp S M and Brader J M 2022 *J. Chem. Phys.* **157** 234108

[102] Tschopp S M, Vuijk H D and Brader J M 2023 *J. Chem. Phys.* **158** 234904

[103] Bickmann J, Bröker S, Jeggle J and Wittkowski R 2022 *J. Chem. Phys.* **156** 194904

[104] Nourhani A, Lammert P E, Borhan A and Crespi V H 2013 *Phys. Rev.* E **87** 050301

[105] Chan C W, Wu D, Qiao K, Fong K L, Yang Z, Han Y and Zhang R 2024 *Nat. Commun.* **15** 1406

[106] van Damme R, Rodenburg J, van Roij R and Dijkstra M 2019 *J. Chem. Phys.* **150** 164501

[107] Dhont J K G 1996 *An Introduction to Dynamics of Colloids* vol 2 (Elsevier)

[108] Redner G S, Hagan M F and Baskaran A 2013 *Phys. Rev. Lett.* **110** 055701

[109] Liu Q X, Doelman A, Rottschäfer V, de Jager M, Herman P M J, Rietkerk M and van de Koppel J 2013 *Proc. Natl. Acad. Sci.* **110** 11905–10

[110] Wysocki A, Winkler R G and Gompper G 2014 *Europhys. Lett.* **105** 48004

[111] Caballero F D, Nardini C and Cates M E 2018 *J. Stat. Mech.* 123208

[112] Cahn J W and Hilliard J E 1958 *J. Chem. Phys.* **28** 258–67

[113] Desai R C and Kapral R 2009 *Dynamics of Self-Organized and Self-Assembled Structures* (Cambridge University Press)

[114] Liao G J and Klapp S H L 2018 *Soft Matter* **14** 7873–82

[115] Wittkowski R, Tiribocchi A, Stenhammar J, Allen R J, Marenduzzo D and Cates M E 2014 *Nat. Commun.* **5** 4351

[116] Zakine R, Simonnet É and Vanden-Eijnden E 2023 arXiv:2309.15033v1

[117] O'Byrne J 2023 *Phys. Rev.* E **107** 054105

[118] Zwicker D 2020 *J. Open Source Softw.* **5** 2158

[119] Thomsen F J, Rapp L, Bergmann F and Zimmermann W 2021 *New J. Phys.* **23** 042002

[120] Fruchart M, Hanai R, Littlewood P B and Vitelli V 2021 *Nature* **592** 363–9

[121] Frohoff-Hülsmann T and Thiele U 2021 *IMA J. Appl. Math.* **86** 924–43

[122] Peruani F, Deutsch A and Bär M 2008 *Eur. Phys. J. Spec. Top.* **157** 111–22